**ISTANBUL TECHNICAL UNIVERSITY ★ GRADUATE SCHOOL OF SCIENCE ENGINEERING AND TECHNOLOGY**

# DEVELOPMENT OF A BIOFUEL CELL CATHODE BASED ON IMMOBOLIZED ENZYMES AND CARBON NANOTUBE (CNT) FOR OXYGEN REDUCTION REACTIONS

**M.Sc. THESIS**

**Ilyas DZHABARLY**

**Department of Chemistry**

**Chemistry Programme**

**JANUARY 2013**

**ISTANBUL TECHNICAL UNIVERSITY ★ GRADUATE SCHOOL OF SCIENCE ENGINEERING AND TECHNOLOGY**

# DEVELOPMENT OF A BIOFUEL CELL CATHODE BASED ON IMMOBOLIZED ENZYMES AND CARBON NANOTUBE (CNT) FOR OXYGEN REDUCTION REACTIONS

**M.Sc. THESIS**

**Ilyas DZHABARLY**
**50909073**

**Department of Chemistry**

**Chemistry Programme**

**Thesis Advisor: Prof. Dr. Figen KADIRGAN**

**JANUARY 2014**

**İSTANBUL TEKNİK ÜNİVERSİTESİ ★ FEN BİLİMLERİ ENSTİTÜSÜ**

# OKSİJEN İNDİRGENME REAKSİYONLARINDA KULLANILMAK ÜZERE KARBON NANOTÜP ÜZERİNE SABİTLENMİŞ ENZİMLERİ İÇEREN BİYO YAKIT PİLLERİ İÇİN KATOT GELİŞTİRMESİDİR

**YÜKSEK LİSANS TEZİ**

**Ilyas DZHABARLY**
**509091073**

**Kimya Anabilim Dalı**

**Kimya Programı**

**Tez Danışmanı: Prof. Dr. Figen KADIRGAN**

**OCAK 2014**

**Ilyas Dzhabarly**, a **M.Sc.** student of ITU **Graduate School of Science Engineering and Technology** student ID **509091073**, successfully defended the **thesis** entitled "**DEVELOPMENT OF A BIOFUEL CELL CATHODE BASED ON IMMOBOLIZED ENZYMES AND CARBON NANOTUBE (CNT) FOR OXYGEN REDUCTION REACTIONS**", which he prepared after fulfilling the requirements specified in the associated legislations, before the jury whose signatures are below.

| | | |
|---|---|---|
| **Thesis Advisor :** | **Prof. Dr. Figen KADIRGAN**<br>İstanbul Technical University | ..... |
| **Jury Members :** | **Prof. Dr. Birsen DEMİRATA**<br>İstanbul Technical University | ..... |
| | **Prof. Dr. Yücel ŞAHİN**<br>Yıldız Technical University | ..... |

**Date of Submission : 16 December 2013**
**Date of Defense : 23 January 2014**

***To my family and my friends***

**FOREWORD**

First of all I would like to express my gratitude to Prof. Dr. Figen KADIRGAN for her guide and support on the course of this entire project.
For all the precious information I learned I would like to thank all scientists that studied in this field and shared their knowledge.
I am also grateful to Pier Parpot for good ideas and advices he gave me at experimental stage of this project.
And of course, thanks to my dear family, my wife and my friends for their support.

December 2013

Ilyas DZHABARLY
Chemistry

**TABLE OF CONTENTS**

**Page**

**ABREVIATIONS**

| | |
|---|---|
| **LAC** | **:** Laccase |
| **BOD** | **:** Bilirubin Oxidase |
| **SW-CNT** | **:** Single Walled Carbon Nanotube |
| **CV** | **:** Cyclic Voltammetry |
| **BFC** | **:** Biological Fuel Cell |
| **MFC** | **:** Microbial Fuel Cell |
| **EFC** | **:** Enzyme Fuel Cell |
| **bmCuO** | **:** Blue Multi-copper Oxidase |
| **TvL** | **:** Trametes Versicolor Laccase |
| **MvBOD** | **:** Myrothecium Verrucaria BOD |
| **ABTS** | **:** 2,2'-azino-bis(3-ethylbenzothiazoline-6-sulphonic acid) |
| **PVP** | **:** Polyvinylpyrrolidone |
| **RDE** | **:** Rotating Disk Electrode |
| **ORR** | **:** Oxygen Reduction Reaction |
| **DMF** | **:** Dimethyl Formamide |

## LIST OF TABLES

**Page**

**LIST OF FIGURES**

**Page**

**DEVELOPMENT OF A BIOFUEL CELL CATHODE BASED ON IMMOBOLIZED ENZYMES AND CARBON NANOTUBE (CNT) FOR OXYGEN REDUCTION REACTIONS**

## SUMMARY

In the worldwide growing demand for the energy resources, fuel cells play an essential role. Many types of fuel cells are being used from huge power plants to microscopic pacemakers. Each of fuel cell has its own characteristic and advantage. Although biological fuel cells express less current values when compared to fuel cells that utilize conventional catalyst, they are more specific and not subjected to poisoning by carbon monoxide.

Biological fuel cell research mostly divided into two parts, anode research and cathode research. While anode based research are focused on utilizing the most proper substrate and building best anode layout, cathode researches focused on oxygen reduction using enzymes, microorganism and that will occur at high potentials and will have high current values.

In this study two enzymes, Laccase and Bilirubin Oxidase, were immobilized on the electrode. These two members of blue multi copper family have two active centers that participate in oxygen reduction reactions. Thus reduction current occurs in two places. However, position, in which enzyme is immobilized plays an essential role as it enables passage of oxygen and electrons to enzyme active center.

In order to increase surface are of the electrode and create proper tunneling environment for enzymes, single wall carbon nanotubes (SW-CNT) were utilized. Carbon nanotubes are known for their conductive characteristics. However, due to their hydrophobic nature, there is an issue arises when enzymes are immobilized on it. To prevent this, PVP was used to modify hydrophobic nature of SW-CNT.

The activity of enzymes was measured both spectrophotometrically and electrochemically. Firstly, kinetics of enzymes that are free in solutions measured, afterwards immobilized enzymes kinetics was measured. Spectrophotometric and electrochemical results were compared to each other. Results were found to be approximately the same. Efficiency drop, hydrogen peroxide effect and PVP coating were analyzed in the study. It was found that enzymes kinetics dramatically decrease with the time. Hydrogen peroxide did not have positive impact on electrode surface, while PVP prevented process of ORR, what was reflected on CV.
To calculate diffusion role in fuel cell, RDE technique was used. Somehow, from the CV obtained, it was concluded that rotation of disk somehow disturbs the surface of electrode and results does not fit RDE rules.
Key Words: Biofuel cell, Single walled Carbon nanotube, Laccase, Bilirubin oxidaze

# OKSİJEN İNDİRGENME REAKSİYONLARINDA KULLANILMAK ÜZERE KARBON NANOTÜP ÜZERİNE SABİTLENMİŞ ENZİMLERİNİ İÇEREN BİYO YAKIT PİLLERİ İÇİN KATOT GELİŞTİRMESİDİR


## ÖZET

Dünya ekonomisinin sürekli gelişmesi ile birlikte ortaya çıkan en büyük sorun enerji kaynaklarının yetersiz olmasıdır. Son yüzyılda pek çok farklı enerji kaynakları bulunmuştur. Bu enerji kaynaklarından bir tanesi de yakıt pilleridir. Diğer enerji kaynakları ile kıyaslandığında yakıt pilleri çok daha verimli ve ekonomiktir aynı zaman da yakıt pillerinin doğaya zarar vermemesi en önemli avantajıdır.

Günümüzde birçok farklı yakıt pili vardır. Bu yakıt pillerinin bazıları yüksek sıcaklıkta, bazılar ise oda koşullarında çalışmak için tasarlanmıştır. Çok farklı boyutlarda yakıt pilleri mevcuttur. Bazıları küçük bir elektrik santrali boyutundadır, bazılar ise mikroskobik ölçekte olup vücudun içerisine yerleştirilebilmektedir. Dolaysıyla, her çeşit yakıt pillerinin yapımında kullanılan malzemeler de farklıdır. Yüksek sıcaklıkta çalışan yakıt pillerinde seramik esaslı malzemeler kullanılır. Oda sıcaklığında çalışan pillerde aktivasyon enerji bariyerini aşmak ve verimliliği artırmak için metal katalizörler kullanılır. Bu yakıt pillerinin en büyük dezavantajı kullanılan metal katalizörlerin pahalı olması, katalizleme işlemi sırasında ortamda bulunan karbon monoksit türevi gazların metal katalizöre inhibitör gibi davranması ve metal katalizörün reaksiyon için spesifik olmamasıdır. Bu sorunları çözmek için çeşitli metal alışımla katalizörler kullanılabilir.

Biyoyakıt pilleri canlı mikroorganizmaları ve bu mikroorganizmalardaki molekülleri kullanmaktadır. Mesela, mikrobiyal yakıt pilleri katotta veya anottaki mikroorganizmalarda gerçekleşen reaksiyonların sonucunda çıkan ürünleri kullanır.

Anotta ya da katotta katalizör olarak enzim kullanılırsa, bu yakıt pili enzim yakıt pili olarak adlandırılır. Bazı durumlarda ise hem anotta hem de katotta enzim kullanılmaktadır. Enzimlerin en büyük avantajı, substrata özel olmasıdır. Bu yüzden seçici bir membrana gerek kalmaz. Ancak, enzim yakıt pilleri çok düşük akım üretir, dolaysıyla verimi düşüktür. Bunun yanı sıra enzimin konumu ve pozisyonu da önemlidir. Enzim yakıt pillerinin en büyük dezavantajı kısa ömürlü olmasıdır. Bu da enzim yapısındaki metallerin aktivitesini yitirmesinden kaynaklanmaktadır.

Bütün yakıt pillerinde en önemli etkenlerden birisi aktif yüzey alanıdır. Yüzey alanı artırmak için karbon nanopartiküller, nanofiberler ya da nanotüpler gibi malzemeler kullanılmaktadır. Bu çalışmada, aktif yüzeyi artırmak amacıyla tek duvarlı karbon nanotüp kullanıldı. Karbon nanotüp elektrotta geniş aktif yüzey alanı oluşturup, elektronlar için serbest geçiş alanı oluşturdu. Bu da, uygun pozisyonda veya konumda bulunmayan enzimlerin aktif olma olasılığını yükseltti.

Bu deneyde, katalizör olarak iki çeşit enzim kullanıldı: lakkaz ve bilirubin oksidaz. Bu enzimler mavi multi-bakır enzim ailesine aittir. Yani, bunların aktivite gösteren bölgelerinde bakır atomları bulunmaktadır. Her iki enzimin yapısı birbirine büyük oranda benzerdir, aktivite bölgeleri ise aynıdır. Bu da bize karşılaştırmalı çalışma imkanı sağlar. Bu enzimler camsı karbon yüzeyine adsorbe olmuş karbon nanotüp üzerine immobilize edildi. Bu konumda enzimlerin aktivitelerine bakıldı.

Kullanılan enzimlerde iki aktif bölgesi vardır. Birinci bölgede substratlar kabul olur, diğer bölgede ise elektronlar. Her iki adımda da bakır atomları büyük rol oynar.

Deney esnasında enzimlerin aktivitelerini yitirmemeleri için tüm hazırlık aşamaları önceden yapılır. Enzimlerin deney dışındaki aktivitelerini inhibe etmek için ve stabil bir saklama ortamı oluşmak için fosfat tampon çözeltisi hazırlandı ve enzimler bu çözeltide saklandı.

Karbon nanotüplerin elektrot yüzeyindeki homojen dağılımını elde etmek için karbon nanotüpler ilk önce dimetilformamit çözeltisinde çözüldü. Daha sonra üç saat boyunca ultrasonik banyosunda bekletildi. Karbon nanotüp solüsyonu elektrot yüzeyine damlatılır ve on beş dakika boyunca azot gazın altında bekletilir. Adsorbe olmayan karbon nanotüpler asetat tampon çözeltisiyle yıkandı. Böylece enzim için yüzey alanı yüksek olan bir zemin hazırlandı.

İlk adım olarak, spektrofotometrik ölçümler alınır. Bu ölçümlerde indikatör olarak ABTS molekülü kullanıldı. ABTS molekülü mavi-bakır enzimlerin ailesinin aktivitelerini gözlemek için kullanılan bir yapıdır. ABTS oksitlendiğinde ABTS radikal katyona dönüşür. Bu değişim 420 nm dalga boyunda gözlenebilir. Spektrofotometrik ölçümleri iki adımdan oluştu. İlk adımda enzimler serbest olarak elektrolitin içinde bulundu, ikinci adımda ise karbon nanotüplü elektrot yüzeyinde sabitlenmiş yapısındaydı. Her iki enzim için ayrı ölçüm alındı ve oluşan farklar gözlemlendi.

Çıkan sonuçlara göre, lakkaz enzimin serbest konumunda bilirubin oksidaz enziminden ABTS molekülünü daha hızlı oksitlenmektedir. Ancak elektrot yüzeyine sabitlendiğinde lakkaz enzimi ABTS molekülünü bilirubin oksidaz enziminden 2.35 kat daha yavaş oksitledi. Bu sonuç lakkaz enzimin pozisyon ve konumuna daha bağlı olduğunu ispatlanmaktadır.

Elektrokimyasal analizinde en çok döngüsel voltametri tekniği kullanılmıştır. Çeşitli tarama hızlarında ve potansiyel aralıklarında yükseltgenme ve indirgenme piklere bakıldı. İlk önce tek duvarlı karbon nanotüp yüzeyine adsorbe olmuş bilirubin oksidaz reaksiyon voltammetrisine bakıldı. Daha sonra aynı işlem lakkaz enzimine uygulandı. Çıkan döngüsel voltamogramlar birbiriyle karşılaştırıldı. Her iki enzim için iki katodik ve bir anodik pik gözlemlendi. İki katodik pik oksijen indirgenme reaksiyonun iki aşamada oluştuğunu göstermektedir. Eksik anodik pik ise yükseltgenme reaksiyon basamağının diğer basamaklarla kıyaslandığında daha hızlı oluşması anlamına gelmektedir.

Lakkaz enzim voltammogramda gözlemlenen düşük akım değerleri lakkaz enzimlerin çok küçük kısmının aktif olduğunu göstermektedir. Bu sonuç lakkaz enzimin konumuna ve pozisyonuna daha bağlı olduğunu bir daha göstermektedir.

Bilirubin oksidaz enzimin voltammogramına bakıldığında daha büyük ve net pikler gözlenmektedir. Bu sonuç bilirubin oksidaz enzimin konumuna ve pozisyonuna daha az bağlı olduğunu gösterdi. Sonuç olarak elektrokimyasal ve spektrofotometrik sonuçlar birbirine benzerdir.
Enzimler ve hidrofobik karbon nanotüp arasındaki etkileşimini geliştirmek için polivinilpirolidon kullanıldı. Bu molekül karbon nanotüpteki hidrofobik özelliğini ortadan kaldırıp daha hidrofilik yapısına dönüştüreceğine beklendi. Ancak beklenen sonuç alınmadı. Bu da, polivinilpirolidonun film oluşturup elektron ve substrat akışı için gereken tünellerinin tıkanmasından kaynaklanabildiğini inanıldı.
Randles-Sevcik denkleme göre, taranma hızı ve pik yükseklikler arasındaki bağlantı araştırıldı ve spektrofotometrik sonuçlar ile karşılaştırıldı. Çıkan sonuçlara göre lakkaz enzimin aktivitesi bilirubin oksidaz enzimin aktivitesine oranı 1:2.27 (spektofotometrik) ve 1:2.35 (elektrokimyasal).

Lakkaz enzimine daha fazla oksijen ulaştırmak amacı ile hidrojen peroksit kullanıldı. Hidrojen peroksit hem oksijen hem de elektron kaynağı olarak kullanılabilir. Ancak, hidrojen peroksit kullanıldığında farklı pikler gözlemlendi. Bu da, hidrojen peroksitin elektrot yüzeyinde reaksiyona girdiğini anlamına gelmektedir. Daha yüksek konsantrasyonlarda ise hiç pik gözlemlenmedi. Bu da, hidrojen peroksitin elektrot yüzeyine adsorbe olan karbon nanotüp ve enzimlerin ayrışmasına sebep olduğunu göstermektedir.

Enzim kinetiğine bakıldığına, bazı varsayımları yaparak ve spektrofotometrik ile elektrokimyasal sonuçları değerlendirerek difüzyon ile enzimlerin aktivite katsayıları arasındaki benzerlikler araştırıldı. Daha sonra çeşitli formulasyon sonucunda deneysel ile teorik sonuçlar karşılaştırıldı.
Son olarak, enzimlerin aktivitelerindeki düşüşü araştırıldı. Alınan sonuçlara göre, fosfat tampon çözeltisinde saklanan enzimlerin aktivitesi beş gün içerisinde %70-80 düşüş gözlemlendi.

Anahtar Kelimeler: Biyoyakıt Pilleri, Lakkaz, Bilirubin oksidaz, Tek Duvarlı Karbon Nanotüp

## 1. INTRODUCTION

The economical progress of any country is strictly related the energy resources. In order to expand the role of energy influence many governments invest money into the field of alternative energy. The main "boom" of alternative energy resources began in the middle of 20$^{th}$ century. New devices, such as fuel cells, solar cells and wind mills, came into being and started to meet energy demand of continuously growing population [1].

Fuel cells were proposed to gain a wide application in many fields, beginning from transportation, aerospace, portable devices, micro power sources and power plants. Compared to conventional energy source, like natural gas, petroleum and coal, fuel cell offers advantages like higher efficiency, harmless reaction products, low or no air and noise pollution [2]. There are many types of fuel cells based on electrolyte, cathode and anode reactants and working conditions.

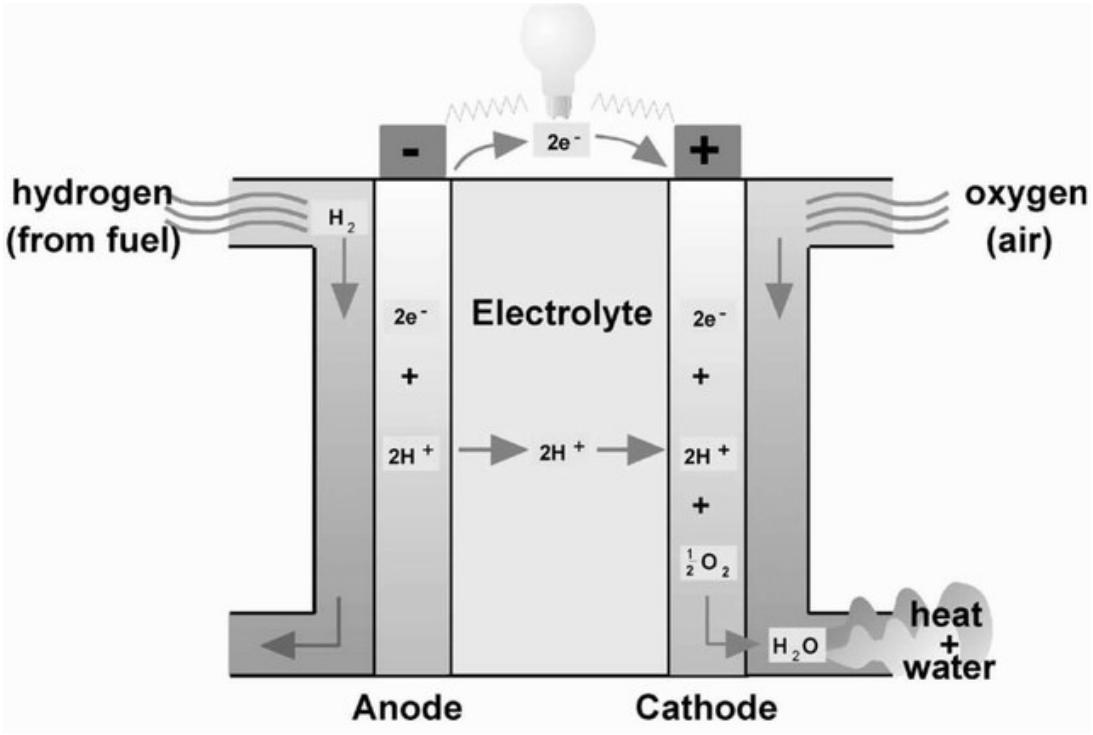


**Figure 1.1**: Fuel cell general scheme.

However, general scheme of it remains the same; anode that is fueled generally by hydrogen or natural gas, cathode supplied by pure oxygen or air and an electrolyte between them to ensure proper pass of ions. Generally, heat and water are the products of fuel cell reaction.

Depending on the environment and desired outcome, various fuel cell types are implemented. However, every fuel cell has its own characteristics which limit its use (Table 1.1).

**Table 1.1:** Fuel cell types and its properties.

| Fuel Cell Type | Advantages | Disadvantages |
|---|---|---|
| Polymer Electrolyte Membrane (PEM) | ● Low startup<br>● Quick start-up<br>● Solid electrolyte reduces corrosion and electrolyte management issues | ● Expensive catalysts<br>● Sensitive to fuel impurities<br>● Low temperature waste heat |
| Alkaline (AFC) | ● Cathode reaction faster in alkaline electrolyte, leads to high performance<br>● Low cost components | ● Sensitive to CO2 in fuel and air<br>● Electrolyte management |
| Phosphoric Acid (PAFC) | ● Higher temperatures enables CHP<br>● Increased tolerance to fuel impurities | ● Pt catalyst<br>● Long start-up<br>● Low current and power |
| Molten Carbonate (MCFC) | ● High efficiency<br>● Fuel flexibility<br>● Ability to implement a variety of catalysts<br>● Suits for CHP implementation | ● High temperature causes corrosion and breakdown of cell components<br>● Long start-up<br>● Low power density |
| Solid Oxide (SOFC) | ● High efficiency<br>● Fuel flexibility<br>● Ability to implement a variety of catalysts<br>● Suits for CHP and CHHP implementation<br>● Hybrid/GT cycle<br>●Solid electrolyte | ● High temperature causes corrosion and breakdown of cell components<br>● Long start-up<br>● Time limits due to high temperature |

For low temperature fuel cell the biggest disadvantage is catalyst costs and operation. Presently, a lot of researches carried out on improving catalyst costs by using composite metals like Pt-Ni, Pt-Co, Pt-Cu etc. [3] In order to increase reactive surface area of catalysts and ensure safe and proper environment for redox

mechanisms, carbon based materials like carbon nanoparticles (Vulcan), nanofibers, grapheme sheets and carbon nanotubes are used. However, although there are many successful results of latter researches, formation of byproducts and catalyst poisoning cannot be overcome totally [4,5].

For high temperature fuel cell the biggest disadvantage is heat management and corrosion of materials of the fuel cell. On the other hand it has a good current generation capability [7].

Biologically compatible fuel cells were offered as a device that could generate electricity from the immersed environment in ambient and natural conditions. Despite short life and low power output, biofuel cells offer advantages like high substrate specificity and absence of membrane between anode and cathode that decreases resistance of an electrolyte. Biological fuel cells (BFC) are mainly divided into two groups: microbial fuel cells (MFC) and enzymatic fuel cells (EFC) [7].

Microbial and enzymatic fuel cells use microorganisms and enzyme respectively to generate electricity from the oxidation of the substrate and concomitant reduction of oxygen to water in mild environment. In some case a hybrid BFC is used e.g. cathode implements oxygen reducing enzyme while anode is Nickel based.

Microbial fuel cells are applicable in a sustainable wastewater treatment technology in autonomous regime. In addition microorganisms are able to oxidize a substrate (e.g. sugar) to CO2 (final product of oxidation). However, lag phase of biofilm formation is too long and bacteria cannot function as an isolated culture. In addition to these issues, compared to conventional fuel cells, generated power density is low.

Enzyme fuel cells are applicable to single chamber fuel cells due to high specificity of enzymes that avoids reaction with other molecules. Extensive studies were carried out to investigate reactions between red-ox enzymes and electrodes. Results did not just lead to more certain information about active site properties but also inspired application of enzymes in biosensors, bioreactors and fuel cells that could power up implants [8, 9]. Some members of ‘blue’ Cu oxidase family exhibited efficiency in fast catalyzing of the four-electron O2 reduction, while other enzymes (dehydrogenase family) were identified to catalyze oxidation of substrates like sugar and alcohol. Consequently, it became possible to build fully enzymatic fuel cells in which both oxidation and reduction reactions would be carried out by enzymes at

small overpotentials. One more advantage of enzyme catalysts is that there is no release of intermediates (like peroxide at metal catalysts), that interrupt with environment of a fuel cell. However, enzymes easily lose their activity or go through denaturalization when there is a change in pH, temperature or pressure [10, 11].

Another big disadvantage of enzyme application in fuel cells is that activity center of it is buried deep inside the enzyme structure, thus direct contact cannot be achieved effectively. To overcome this issue, various immobilization techniques are used to electrically communicate enzymes with electrodes. General technique is based on the direct deposition of an enzyme on the electrode surface. There are also four other techniques distinguished. First technique is based on the reconstitution of an apo-enzyme on a relay-cofactor unit bound to the electrode (Fig 2-A), second technique is an immobilization of an enzyme inside the red-ox polymer (red-ox hydrogels) that is associated with electrode surface(Fig 2-B), third one is based on connection of redox-relay units to the protein that is associated with electrode surface(Fig 2-C) and last technique is based on use of diffusional electron mediator(Fig 2-D).

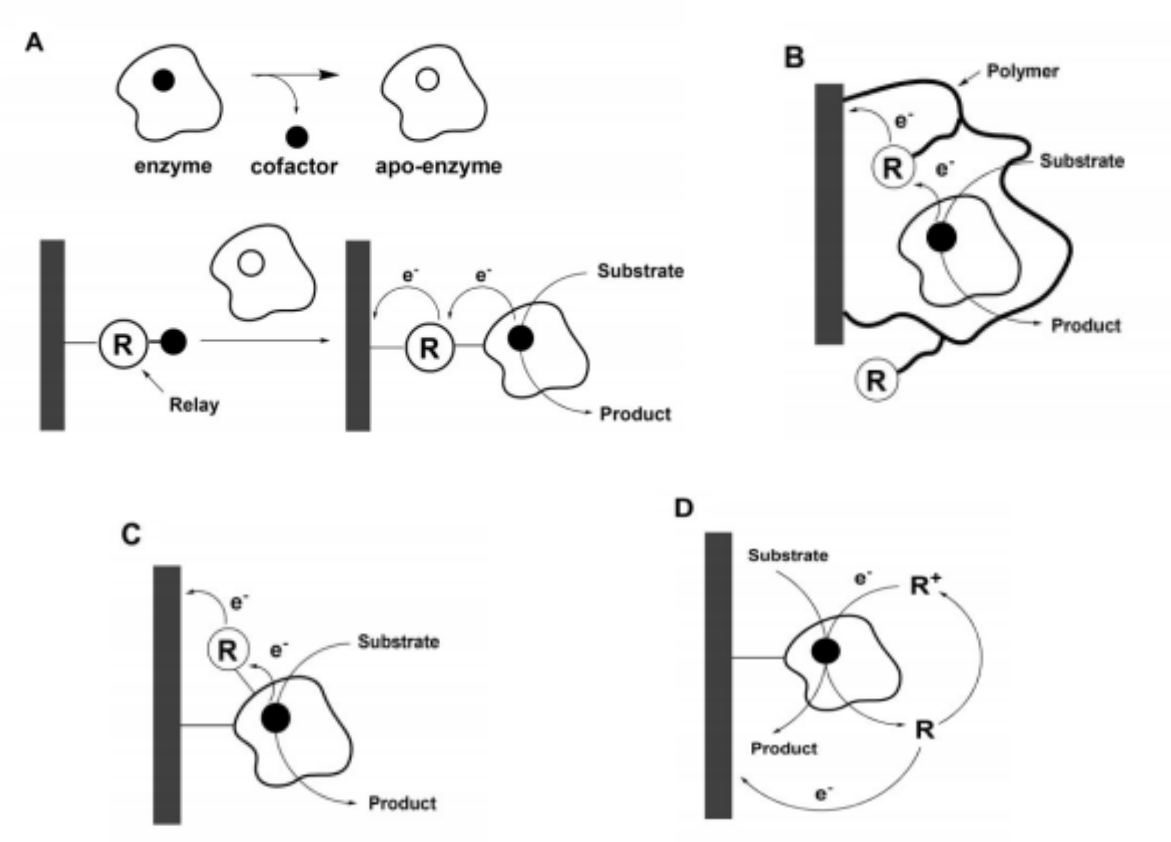


**Figure 1.2:** Techniques of electrical connection of enzymes associated with electrode surface.

Each technique has distinctive characteristics that lead to various positive and negative outcomes [12,8, 13].

Although enzymes offer opportunities like avoiding use of selective membrane and specificity for molecules, it also easily loses activity or denaturizes when any change in pH, temperature or pressure occurs. In addition it is known that activity center of the enzyme is buried deep inside the enzyme structure, consequently the good energy output is achieved only by mediator based transfer. However, mediators are usually expensive and toxic materials, thus it is not desired to facilitate electron transfer by them [9, 14].

## 1.1 Purpose of the thesis

This project was focused on enhancing direct electron transfer by directly deposited enzyme on carbon nanotubes (CNT's). Due to its properties, CNT's provide good electron conducting properties and high surface area. This enhances mechanism of red-ox pathway and increases the chance of an enzyme active center to be close to the electroactive surface.

Enzymes used as catalysts are members of 'blue' copper family laccase and bilirubin oxidase. The nature of transfer will be analyzed using various electrochemical and spectroscopic techniques.

## 1.2 General information and Literature review

### 1.2.1 Enzymes Used

#### 1.2.1.1 Laccase

Laccase is a fungal, polyphenol oxidizing enzyme that belongs to the blue multicopper oxidase (bmCuO) family. Enzymes of this family catalyze the four-electron reduction of molecular oxygen to water accompanied with the one-electron oxidation of four reducing-substrate molecules (preferably phenolic compounds) [15].

Members of bmCuO family mainly contain four copper atoms coordinated as three active sites: type -1 (T1), type - 2 (T2) and type - 3(T3) which are classified according to their spectroscopic and electronic properties [17]. T1 is a mononuclear

(contains one copper atom) site and assumed to be responsible for oxidation processes [16]. T2 site is also mononuclear, while T3 site has a binuclear structure in which two Cu (II) atoms are cross-linked by hydroxyl ion. Both of T2 and T3 site form a trinuclear cluster that is presumably responsible for reduction of O2.

The red-ox reaction begins with T1 Cu-center oxidizing the reducing substrate and the subsequent transfer of the generated electrons to the T2 and T3 Cu-centers [17]. In details, the reducing substrate binds to a T1 pocket and reduces Cu(II) to Cu(I), afterwards the generated electron is transferred from T1 to the T2/T3 cluster, where it finally causes reduction of bound O2 to H2O [18,16]. It is proposed that laccase red-ox reaction acts in a "two-site ping-pong bi-bi" manner, meaning that release of products occurs before new substrate is bound. Solvent channels of bmCuOs contribute to quick access of O2 and following easy release of H2O [19, 20].

According to amino acid composition, that causes change in red-ox potential, laccases are divided into two categories: as low (500 mV *vs.* NHE) and high (700–800 mV vs. NHE) E0 laccases [21].

In following experiment laccase from Trametes versicolor (TvL) was used.

### *T. Versicolor* laccase

TvL was first characterized in an active state by Pointek and his group. They were able to screen enzyme with all T1, T2 and T3 sites active (copper ions not depleted state), what was not achieved before for members of bmCuO. [16] Despite some slight differences, the gene LccL is presumed to be responsible for encoding the enzyme [22]. Monomeric TvL structure is based on three sequentially arranged domains, with overall dimension of about 65 × 55 × 45 Å.

As it can be seen on the Figure 1.3, the copper coordination of the whole tri-nuclear cluster (T2/T3) is maintained by the residues of D1 and D3. T2/T3 site is buried at the depth of 12 Å within the molecule [18, 21].

T2/T3 cluster can be accessed via two channels that lead to type-2 and type-3 copper sites ( Fig 1.4). One channels function is to give access for molecular oxygen, while other channel releases formed water molecule. In comparison to T3 site, T2 site is more exposed to the outer environment that is why in an inactive enzyme mostly type - 2 copper is depleted. Along both channels there are water molecules that are connected to surrounding residues by hydrogen bonds [23].

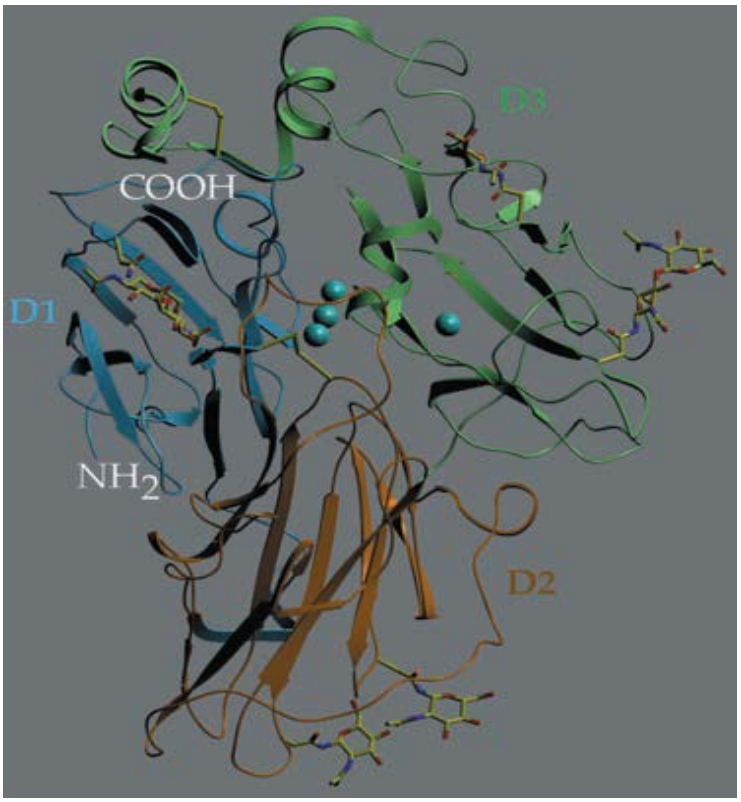


**Figure 1.3:** Ribbon diagram of TvL (Domains of the enzyme (D1-D3) are shown in three different colors. Blue spheres are the copper ions. Stick models express carhobydrates and disulfide bonds.

T1 copper plays the role of a primary electron acceptor. The connection and the electron transfer between T1 and T2/T3 coppers are maintained by His-Cys-His tripeptide. T1 and T2/T3 coppers are located at an average distance of 12 Å [16].

All redox functional sites including tripeptide and both channels are highly conserved. Reoxidation rate of the coppers in TvL is 5 × 106 M −1sec−1. [26, 27] TvL enzyme belongs to high E0 enzymes with a red-ox potential of 800 mV.

#### 1.2.1.1 Bilirubin Oxidase (BOD)

Bilirubin oxidase BOD (bilirubin:oxygen oxidoreductase, EC 1.3.3.5) is a member of a multi-copper oxidase family that catalyze the oxidation of tetrapyrroles, diphenols, aryl diamines and bilirubin to biliverdin, concomitant with reduction of molecular oxygen to water [24].

It is produced by a wide range of living organism including fungi, bacteria and animals. Same as laccase enzyme, BOD enzyme has three active sites (type 1 (T1), type 2 (T2), and type 3 (T3) copper ions) with comprising four copper ions in it.

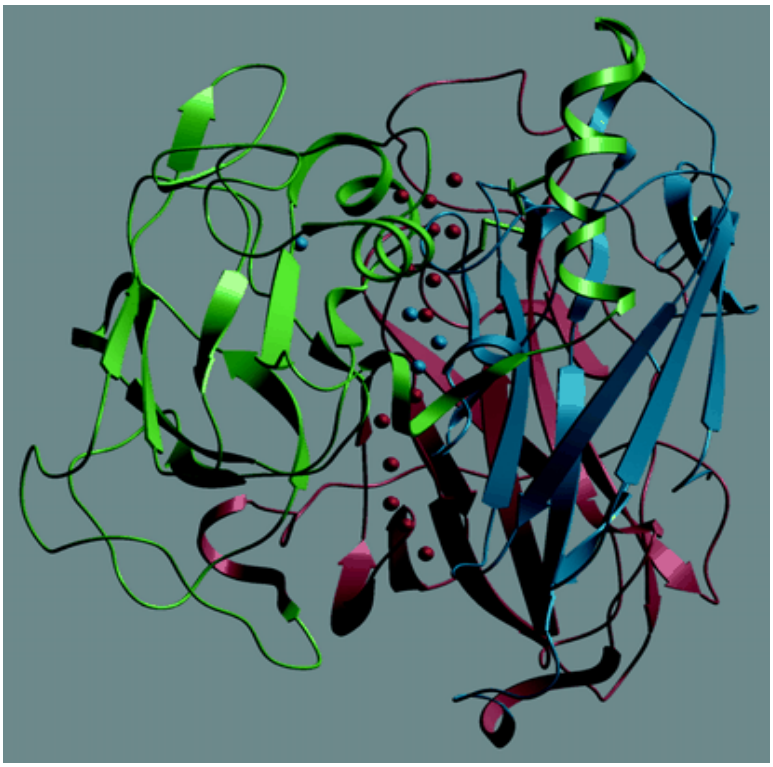

**Figure 1.4:** TvL structure showing that T2/T3 cluster has two access channels. (Copper ions are blue spheres, and water molecules are red spheres).

BOD shows similarity with blue multicopper oxidases by forming the trinuclear cluster from T2 and T3 sites. Latter sites are responsible for reductions of O2 to H2O. T1 site oxidizes the electron donating substrate [25, 18, 16]. Due to special arrangement of four ‘’blue’’ coppers, BOD is counted as a member of blue multicopper oxidases [27].

#### 1.2.1.2.1 Myrothecium verrucaria BOD (MvBOD)

The molecular weight of MvBOD is 52-64 kDa Of these. Like other multicopper oxidases it shows absorbance at 600 and 330 nm [28, 29]. MvBOD T1 copper ligands (two hystidines, a cysteine and a methionine) express identity with ligands of low red-ox potential multicopper oxidases [30]. Consequently, MvBOD (Eo 480 mV) is assumed to belong to the class of low red-ox potential multicopper oxidases. However, there were reports of MvBOD to have high red-ox potentials [31].

In MvBOD the distance between Type 1 Cu site and trinuclear Cu cluster of Type 2 and Type 3 is around 12-13 Å. Same as laccase enzyme, MvBOD Type 1 Cu atom is linked to Type 2 and Type 3 trinuclear Cu cluster by His-Cys-His sequence (Fig 1.5).

Latter sequence maintains electron transfer from the oxidized substrate to molecular oxygen to be reduced [32].

All residual amino acids around active sites of MvBOD are also conserved identically in CotA, Fet3p, CueO, ceruloplasmin, ascorbate oxidase, tree laccase and PcoA.

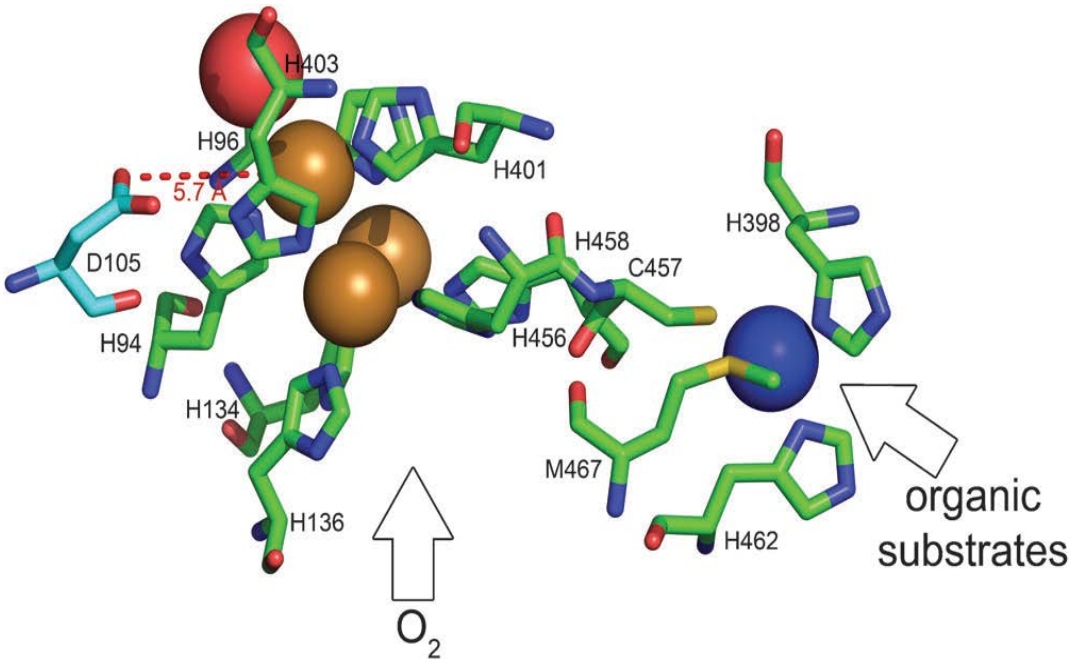


**Figure 1.5:** Three-dimensional structure of MvBOD T1, T2 and T3 active sites. (Protein Data Bank code: 2XLL). **(**Blue sphere represents T1 Cu atom, brown spheres represent T2 and T3 trinuclear Cu cluster, red sphere is a oxygen species bound to trinuclear Cu cluster. During oxygen aspartate (D105) is assumed to donate protons).

The redox reaction pathway of MvBOD is similar to Laccase's one. After electron is obtained from the oxidation of the substrate at T1 Cu, it is transferred to the T2/T3 trinuclear Cu cluster, where it causes reduction of $O_2$ to $H_2O$ [33,31] (Fig 1.6).

According to the detailed spectroscopic catalytic mechanism described by Solomon and his group, two highly active intermediates were revealed. Latter intermediates are produced and take place in the following order:

(a) Peroxy-intermediate (PI) is produced as a result of reaction of O2 and fully-reduced enzyme with a rate constant of 2 x106 M-1 s-1. Although O2 molecule of this intermediate is reduced, O-O bond remains

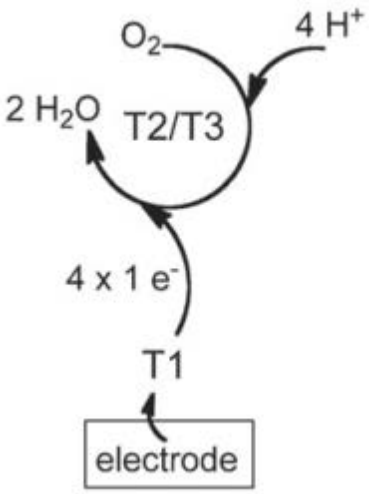


**Figure 1.6:** Redox reaction mechanism of MvBOD.

(b) As a result of reaction of PI ‘’native intermediate’’ (NI) species are produced. In this species all four Cu atoms have 2+ state, while elements of original O2 stay and play the role of oxo and hydroxo bridging ligands of the T2/T3 site

(c) As a result of fast transfer of four electrons and four protons and release of water, enzyme recovers its fully reduced state

There is a huge impact of pH on MvBOD. In pH around 5, MvBOD maintains fast intramolecular processes, T1 redox cycling determines turnover rate (current) and the potential of electrocatalysis is influenced but not defined by T1 red-ox potential. While in pH 8 conditions, there are slow intramolecular processes, which determine turnover rate (current) and the potential of electrocatalysis is totally controlled by T1 redox kinetics [34, 30]. In addition MvBOD demonstrates considerably smaller overpotentials than Pt at neutral pH [35].

### 1.2.2 ABTS

In order to spectrophotometrically analyze enzyme oxidation kinetics ABTS or 2,2'-azino-bis(3-ethylbenzothiazoline-6-sulphonic acid) was used. ABTS is the chemical compound used as the tool for analyzing reaction kinetics of blue-multicopper family member enzymes. When oxidized, ABTS turns into its colored radical cation (ABTS● +) that absorbs light at 420 nm. ($\varepsilon = 3.6 \times 10^4\ M^{-1}\ cm^{-1}$) Absorbance change with the amount of cation formed, thus absorbance directly reflects kinetics of the enzyme used [36].

### 1.2.3 PVP

PVP ((C6H9O)n, MM 2.500-2500000 g/mol) or Polyvinylpyrrolidone (PVP) is a water soluble polymer that is made of N-vinylpyrrolidone monomer in the process of radical polymerization. Firstly synthesized by Walter Reppe 1930's. Due to its excellent wetting properties it is used to form films and change hydrophobicity of the surface. In addition it makes good coatings or can be used as an additive to coating agents [37].

### 1.2.4. Electrochemical Methods

#### 1.2.4.1 Cyclic voltammetry

Cyclic voltammetry is a method investigating electrochemical behavior of the whole system. It gives qualitative information about electrochemical reactions and provides a clear sight at red-ox potentials of electroactive species. The measurement based on the working electrode potential that is ramped linearly from initial potential Ei to final potential Ef. Afterwards, when Ef is reached, reverse step takes place and potential goes back from Ef to Ei (Fig 1.7). Sweep rate varies from a few milivolts per second to hundred volts per second.

As a result, cyclic voltammogram is obtained, on which current behavior against potential applied is monitored (Fig 1.8). The current measured is often normalized to the surface area of the electrode and named current density.

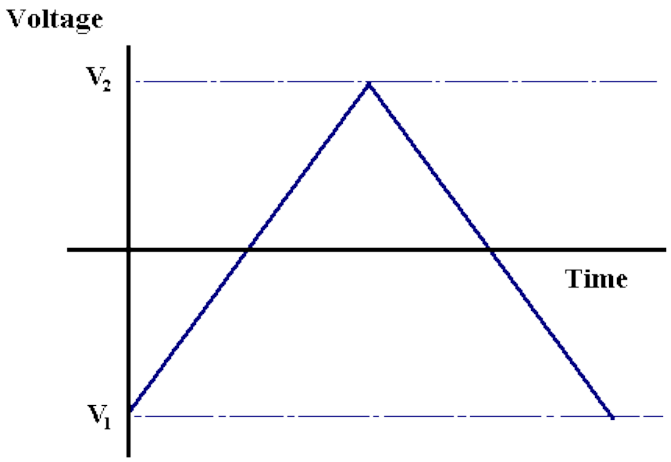


**Figure 1.7:** CV potential change within a time.

Current change is associated with species red-ox activity. The peak current ip of the voltammogramm can be expressed by the Randles-Sevcik equation (1.1):

$$i_p = (2.687x10^5)\, n^{3/2}\, v^{1/2}\, D^{1/2}\, A\, C \qquad at\ \ 25\ °C \qquad \textbf{(1.1)}$$

where n is the number of electrons transferred, A is the electrode area, D is the diffusion coefficient of the analyte, v is the scan rate and C* is the bulk concentration of the analyte. Peak current increases with higher scan rate [38].

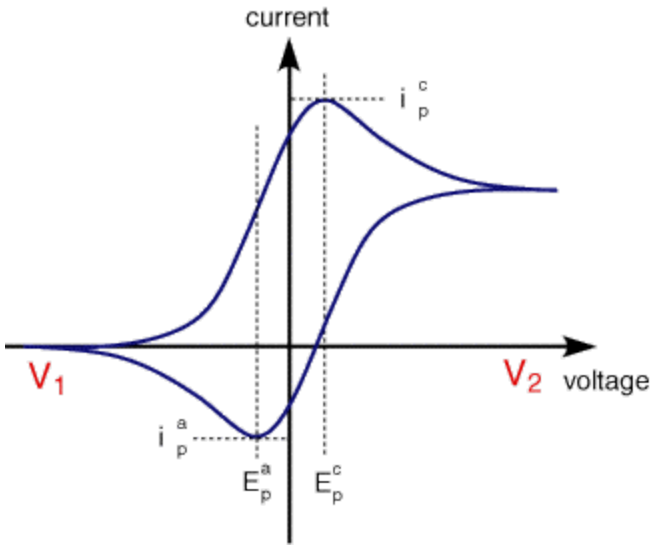


**Figure 1.8:** Cyclic voltammogram.

## 2. MATERIALS AND METHODS

### 2.1 Methods and Used Equipment

For electrochemical measurements carried out in the experiment PARSTAT ®2273 advanced electrochemical system (potentiostat) (Fig 2.1) of Princeton Applied Research was used. Directly deposited CNT-Enzyme layers were checked for ORR using conventional CV methods at various scan rates.


**Figure 2.1:** PARSTAT ®2273 Potentiostat.

All electrochemical measurements were carried at 25 $cm^3$ single chamber water jacketed glass cell (Fig 2.2) with separated glass top containing five necks. Water flow enables temperature regulation, while glass top necks serve for oxygen-nitrogen inflow and inflow rate monitoring and three left necks are for working, reference and counter electrodes.

#### 2.1.1 Electrochemical characterization

To analyze the nature of electrochemical interaction between molecular oxygen, enzyme and CNT, electrochemical characterization methods should be employed. The most used amongst them is CV, which provides cyclic voltammogram which

gives clear view on the voltage-current relation, thus revealing every aspect of ORR kinetics.


**Figure 2.2:** Glass cell with compartments: 1) Working electrode, 2) Reference Electrode, 3) Counter electrode, 4) Oxygen-Nitrogen inflow hose, 5) Oxygen-Nitrogen monitoring compartment, 6) Water jacket inflow-outflow hoses.

CV voltammogram can be analyzed according to Randles-Sevcik equation **(2.1)** which describes peak height ($i_p$) in amperes (A) in the following way;

$$i_p = 0.4463\ n\ F\ A\ C\ (n\ F\ v\ D\ /\ R\ T)^{1/2} \qquad \textbf{(2.1)}$$

where n is the number of electrons, F is Faraday's Constant (96485 C/mol), A is the electrode area, D is the diffusion coefficient, C is the concentration, R is the universal gas constant (8.314 J/mol K), T is the absolute temperature (K) and v is the sweep rate.

Using (2.1) equation it is possible to calculate D or diffusion coefficient that plays essential role in the enzyme-CNT based electrodes as it establishes proper transport of molecular oxygen and electron to the active center of an enzyme.

### 2.1.1.1. Working Electrode

Working electrode EDI101of Radiometer Copenhagen (Figure 2.3) was used in this experiment. Removable electrode tip is made of Teflon which does not react with any solution and avoids leakage of inside the electrode. In the center of removable tip there is a core rod of glassy carbon on the tip of which the whole reaction occurs.


**Figure 2.3**: Working electrode 1)Removable tip 2)Rotating stem.

Another advantage of the current electrode is the rotating stem, that allows perform rotation based measurements like Rotating Disk Electrode method. RDE method is based on the controlled and forced convection of the solution to continually deliver material to the electrode.

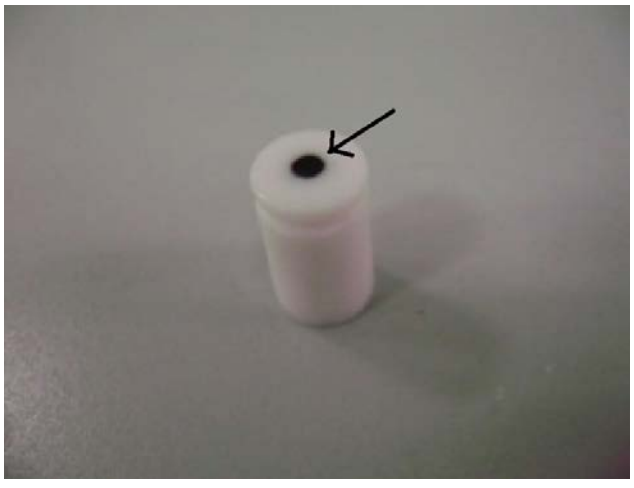

**Figure 2.4:** Working electrode removable tip, arrow point at the glassy carbon rod.

Material of the solution is pulled upward by the vortex flow which is created by rotating stem. As a result, the solution is homogenous. However, next to the

electrode surface the stagnant layer called Levich layer is formed and it sticks and moves with electrode as it rotates. Diffusion type mass transfer occurs inside this layer. As concentration gradient is constant with respect to time on the electrode surface, the current is a steady-state current.

Levich layer thickness depends upon conditions and can be expressed with the following equation;

$$\delta_L = 1.61\, D^{1/3}\, \omega^{-1/2}\, \upsilon^{1/6} \qquad \textbf{(2.2)}$$

where D is the diffusion coefficient (in cm2/s), ω is the rotation speed (rad/s), and υ is the kinematic viscosity (in cm2/s).

If considered that limiting current at the electrode surface is proportional to the thickness of the Levich layer by the following equation;

$$i_l = n\, F\, A\, (D / \delta)\, C \qquad \textbf{(2.3)}$$

where n is the number of electrons in the electrochemical reaction, F is Faraday's constant (96485 C/mol), A is the electrode area (in cm2), and C is the concentration (in mol/cm3).

It is possible to rewrite fully expanded limiting current by the Levich equation in the following order;

$$i_l = 0.62\, n\, F\, A\, D^{2/3}\, \omega^{1/2}\, \upsilon^{-1/6}\, C \qquad \textbf{(2.4)}$$

#### 2.1.1.2. Counter Electrode

Platinum gauze electrode was used in current study. Main function of counter (auxiliary) electrode is to establish two-cathode system. In our case, platinum gauze counter electrode played role of anode, as we were investigating reaction occurring on cathode. Surface area of the counter electrode should be larger than the working electrode area to avoid any limiting half-reaction occurring on the surface of counter electrode. In combination with working electrode, counter electrode forms a circuit through which current is whether applied or measured. Main fabrication materials for counter electrode are electrochemically inert materials like gold, platinum or carbon.

### 2.1.1.3. Reference Electrode

In our study standard calomel electrode $Hg/HgCl_2/KCl$ (NHE 0.244 V) was used. Main function of this electrode is to control potential of the working electrode. Potential difference arises from the following reaction that occurs in the reference electrode:

$$Hg_2Cl_2 + 2e^- \leftrightarrow 2Hg\ (s) + 2Cl^-\ (aqueous)$$

## 2.2. Chemicals Used

As enzymes Bilirubin oxidase from Myrothecium verrucaria (4.5 mg solid, 5.6 units/mg solid, 18 units/ mg protein, SIGMA-Aldrich) and Laccase from Trametes Versicolor ( 13.6 U/mg solid, Sigma-Aldrich) were used, ABTS (2,2'-azino-bis 3-ethylbenzthiazoline-6-sulphonic acid) (Applichem) was used for identification of an enzyme activity, acetic acid and NaOH used to prepare acetate Buffer for electrolyte, $K_2HPO_4$ and $KH_2PO_4$ used to prepare phosphate buffer for enzyme storage, SW-CNT, ≥80.0% (carbon as SWNT, Sigmda-Aldrich) was used as tool to increase surface area for enzyme immobilization, NN-Dimethylformamide (Merck-Suprapur) was used to disperse SW-CNT, $H_2O_2$ was used as additional source of oxygen, Polyvinylpyrrolidone (with an average molar weight 40,000, Sigma-Aldrich) was used to decrease hydrophobic property of SW-CNT, glutaraldehyde solution (%25 in $H_2O$, Sigma-Aldrich) to immobilize enzymes, deionized and distilled water Millipore MilliQ, 18MΩ.cm used in any procedure required.

## 2.3. Methods

### 2.3.1 SW-CNT solution Preparation

SW-CNT powder was dissolved in the DMF with the ration of 1 mg/mL. Then solution is left in ultrasonic bath for 2 hours. Afterwards, homogenous solution was kept cool, dry and dark place.

### 2.3.2 Enzyme Solution Preparation

50 U/mL of BOD solution was prepared using 0.1 M Phosphate Buffer pH 6.4 and stored in cold and dark place. 50 U/mL of Laccase solution was prepared in the same

way as BOD solution and kept in the same conditions. In order to avoid loss of activity of enzymes, ABTS activity measurements were carried right after enzyme preparation. Due to small amount of BOD provided, firstly, experiments using BOD were carried.

### 2.3.3. Spectrophotometric Characterization of Enzyme Activity

In order to obtain valuable information about enzyme activity in the fuel cell, ABTS was used. In order to see the difference between activity of an immobilized enzyme and free enzyme electrode surface simulation using ABTS molecule was performed.

In first step of the simulation, two glass tanks of the same volume as the half cell tank were prepared as following: 25 mL of 0.05 M Acetate buffer pH 4.55 was mixed with 15 µL of 50 µM ABTS and covered with aluminum foil to avoid reactions of ABTS.

In first tank, 10 µL of the enzyme immobilized on the electrode (rotation speed 100 RPM) according to procedure 2.3.4 is inserted and in the second tank with solution, 10 µL was injected directly into the solution (Figure 2.5).

Absorbance was measured on UV-1800 Shimadzu UV-spectrophotometer at 420 nm for a period of 120-250 minutes.

### 2.3.4. Working Electrode Preparation

First of all, after keeping SW-CNT solution in ultrasonic bath for 30 minutes, 5 µL of the solution were injected on the glass carbon electrodes and left for drying under a slight $N_2$ gas blow for 1 hour. Afterwards, electrodes were gently rinsed in 0,05M Acetate Buffer pH 4.55 to remove unadsorbed CNT's. Rinsed electrodes are left to dry for 15 minutes in $N_2$ gas. $N_2$ gas used to avoid adsorption of any unwanted gases to CNT and inhibit reaction of $O_2$ with CNT for the period of electrode preparation.
As secondary electrode modifications, PVP was used to modify hydrophobicity of SW-CNT to establish better connection and electron flow with the enzyme that is applied later on the electrode. 4 µL of 5 mg/ml PVP is added on the electrode and left to dry again under $N_2$ flow.
Thirdly, 5 µL of previously prepared enzyme (Laccase or BOD) is applied on the electrode surface and left to dry for 30 minutes under $N_2$ gas.

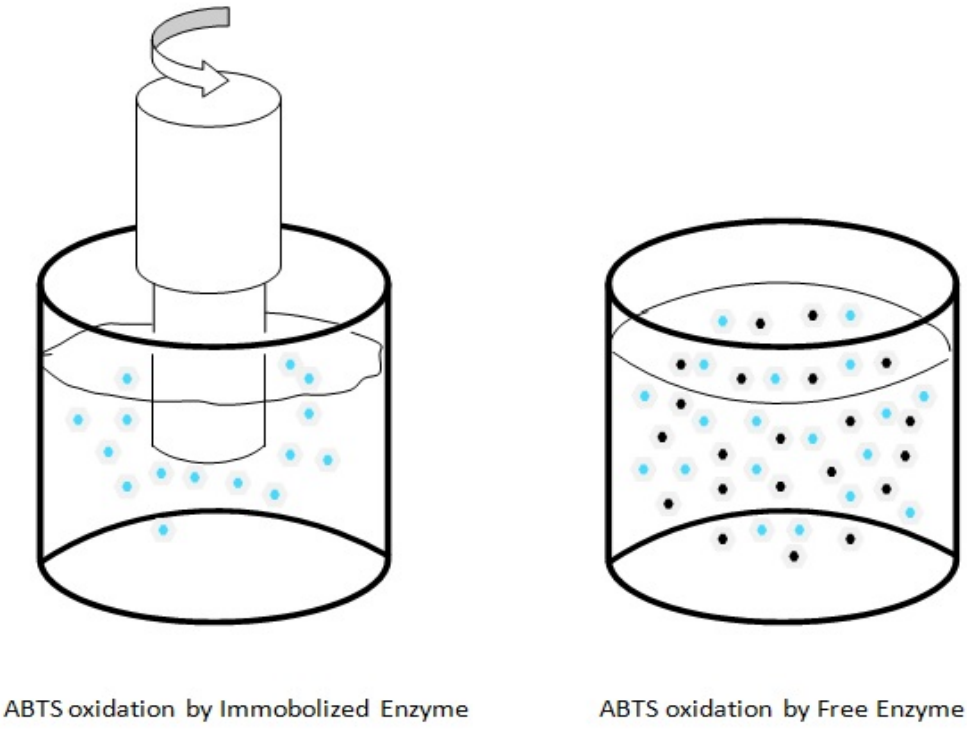


**Figure 2.5:** ABTS oxidation comparison between immobilized enzyme and free enzyme.

Lastly, in order to avoid enzyme washout from the electrode surface 2.5 µL of 0.04 M glutaraldehyde was injected on the electrode "layout" and left to dry under $N_2$ flow.

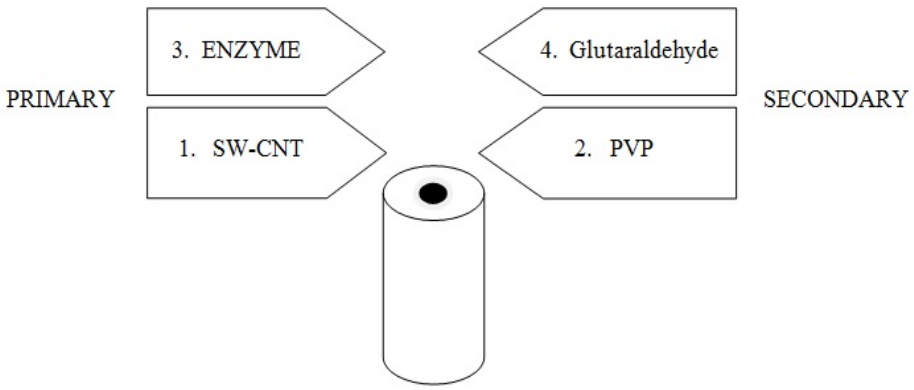


**Figure 2.6:** Electrode preparation layout.

Before measurements, half cell was rinsed with boiling water to remove unwanted absorbed particles. After each measurement, carbon electrode was polished gentle pad with the help of alumina (particle size 1, 0.05 and 0.3 µm**)** FF slurry and rinsed

with Milipore water. In addition, electrode was sonicated between and after polishing for 10 minutes. All the calculations were made according to electrode surface area of 0.071 $cm^2$.

## 3. RESULTS

### 3.1 Spectrophotometric Characterization of Enzymes

From the absorbance plots obtained, it is obvious that free enzyme performance is higher than immobilized one. Absorbance change is the cause of ABTS oxidation to its blue-red cation form $ABTS^{+}$.

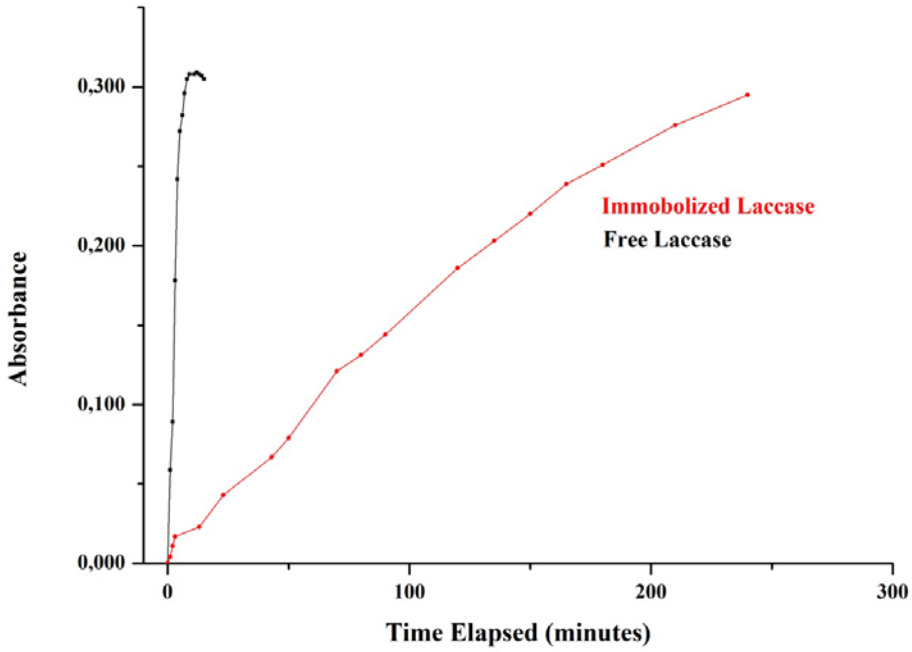


**Figure 3.1:** Absorbance change difference between free laccase (black line) and immobilized laccase (red line), 0.05 M acetate buffer pH 4.55, 20 $^{o}$C.

The more ABTS oxidized the more absorbance rises. ABTS+ amount increases sharp within first 10 minutes with immobilized enzyme that means that free laccase oxidative function is very efficient. As all ABTS is oxidized, absorbance increase stops. While laccase increment profile resembles linear structure (Figure 3.1), BOD increment profiles (Figure 3.2) more or less close to exponential-sigmoidal structure. Linearity of laccase plot makes it easier to analyze the behavior of the laccase in two

different conditions; when laccase is free in solution and when it is immobilized on the surface of the electrode. It is obvious from plots on the Figure 3.1 that with the case of free laccase, absorbance reaches its highest point within less than 12 minutes after which absorbance stays constant for a couple of minutes and starts to drop. It can be due to formation of gas bubbles at late phases.

However, for the immobilized enzyme it takes 250 minutes to reach same absorbance values as free enzyme. From this point, it is easy to conclude that efficiency of immobilized enzyme almost 20 times lower than free enzyme. This can be addressed to two facts about immobilized enzyme. Firstly, it can be resulted from the low diffusion of ABTS molecule to laccase that is immobilized on the surface of the electrode. Secondly, it can be due to improper position of enzyme on the electrode surface in which one of the active sites (T1, T2 or T3) is unavailable for substrate processing. Lastly, there is the possibility of inactivation of enzyme as the result of electrode drying steps and only a few enzymes on the surface active.

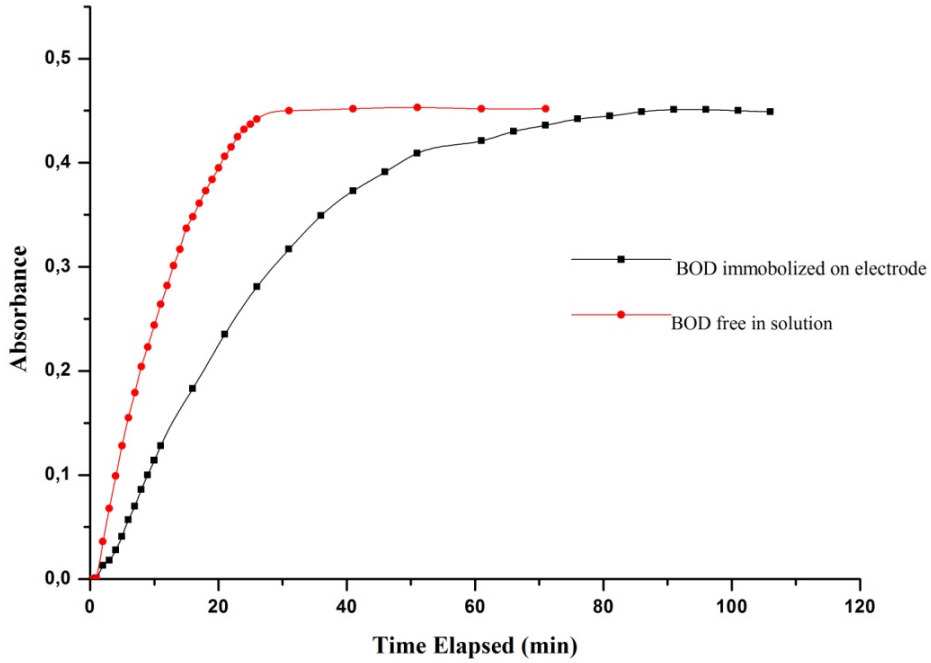


**Figure 3.2:** Absorbance change difference between free BOD (black line) and immobilized BOD (red line), 0.05 M acetate buffer pH 4.55, 20 $^{o}$C.

In case of BOD plots (Figure 3.2) we can see that both plots does not follow linear patters as it was with laccase plots. Instead it represents exponential-sigmoid

increment pattern. Both plots represent relatively slow absorbance increase compared to laccase plots. Free BOD enzyme absorbance reaches its maximum in about 27 minutes (more than two times lower than laccase enzyme) and stays constant for a long period of time with no drop. However, in case of immobilized BOD, maximum absorbance value is reached just in 110 minutes, which is relatively low compared to maximum absorbance reach time of laccase that is also immobilized. It can concluded from here that position of a BOD enzyme is less important than laccasses one.

### 3.2 Electrochemical analysis

#### 3.2.1 BOD electrochemical analysis

Due to small amount of BOD, firstly experiments with BOD were carried to prevent denaturation or loss of functions that can occur within a short period of time. To understand the nature of BOD oxygen reduction behavior, it is essential to have a look at cyclic voltammogram in comparison with the SW-CNT only voltammogram.

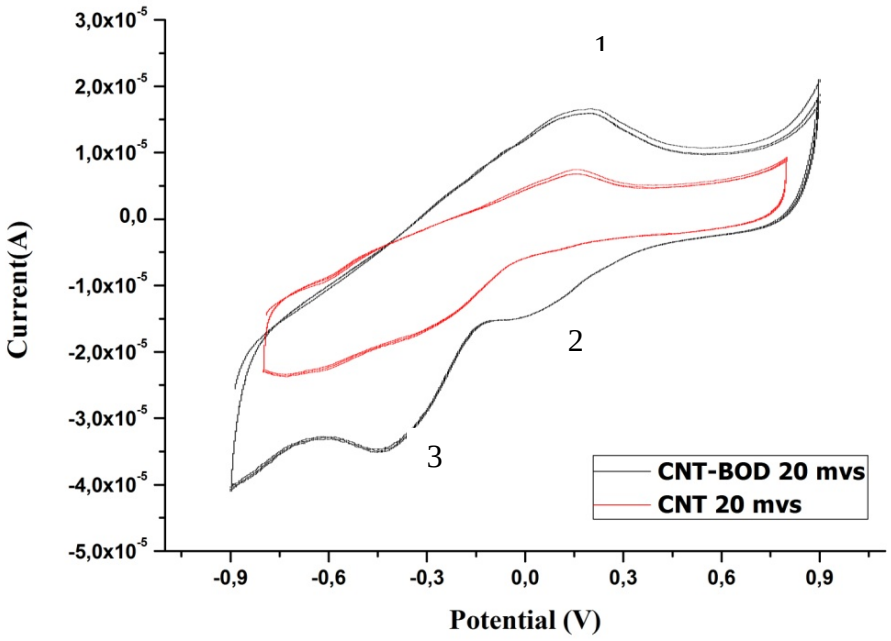


**Figure 3.3:** Cyclic voltammogram of SW-CNT (red) and BOD immobilized on SW-CNT, sweep rate 20 mV/s, 20 $^{0}$C, 0.05 M pH 4.55 Acetate Buffer.

Although it is known that SW-CNT can participate in ORR, from the Figure 3.3 it is seen how BOD immobilized on the SW-CNT has a higher current outcome than SW-CNT alone. First of all, it would be essential to consider the anodic peak of the cyclic voltammogram, in which it is clear that both SW-CNT and BOD-SW-CNT has it. However, BOD-SW-CNT has the higher anodic peak meaning that, more electrons are dragged to enzymes and more oxidative species are formed on the surface of the electrode. As previous studies [12, 13, 20] describe in details; reduction of the oxygen does not occur as single stage reaction. T1 site accepts electrons from the electrode or from the substrate oxidation, at that point Cu atom at T1 site undergoes changes which reflects upon cyclic voltammogram at site 2. As the next stage of ORR; electrons flow through the tunnel in BOD created by His-Cys-His sequence and reach T2-T3 site where the final reduction from $O_2$ to $H_2O$ occurs. The latter stage is reflected on the cyclic voltammogram as site 3 [16, 18].

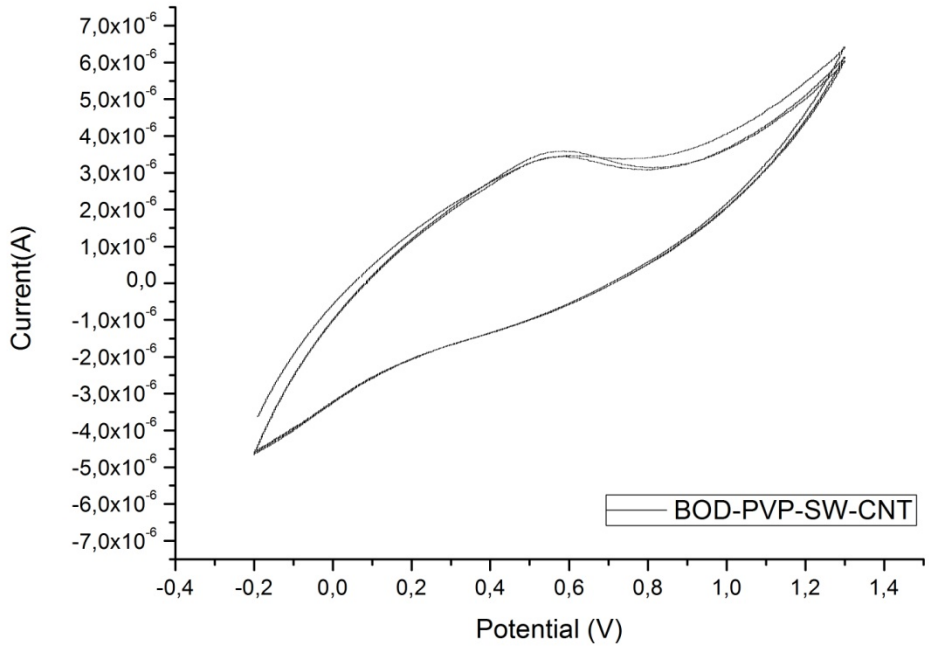


**Figure 3.4:** Cyclic voltammogram of BOD-PVP-SW-CNT layout, 10 mV/s, 20 $^0$C, 0.05 M pH 4.55 Acetate Buffer.

As it is hard to predict the real effective surface area of the enzyme, it is better to take some values theoretically and use some approximation tools.

As it was mentioned before, in order to change hydrophobic nature of SW-CNT PVP was used. As next step BOD was applied on the PVP covered SW-CNT and cyclic voltammogram was taken. On the Figure 3.5, it is seen that BOD behavior on the PVP covered SW-CNT is not clear as it is without PVP. Anodic peak is obvious at around 0.57 V and a slight cathodic peak is seen at the range of 0.3-0.8V. In addition, Figure 3.5 represents overpotential behavior voltammogram. Possibly it can be caused by concentration or resistance overpotential caused by thickness of layers applied on the electrode surface.

In order to have a clear sight of PVP caused overpotential, it is better to compare two voltammograms of BOD-SW-CNT and BOD-PVP-SW-CNT. As it is seen on the Figure 3.5, while in absence of PVP, there are clear and more sharp both anodic and cathodic peaks, in the presence of PVP both peaks are not even obvious on the voltammogram. In addition the incline of that incline is more than incline of the voltammogram without PVP, meaning that overpotential effect reflected more on it. From this, it can be concluded that PVP is not the best agent for the electrode modification in case of use it on SW-CNT-BOD layout.

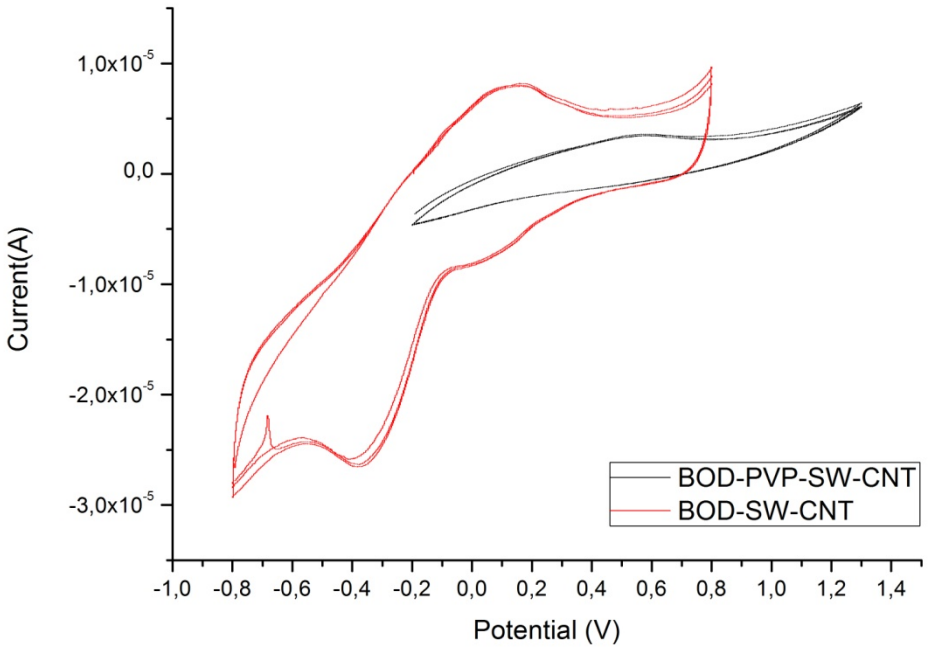


**Figure 3.5:** Cyclic voltammogram comparison of BOD-PVP-SW-CNT and BOD-SW-CNT layouts, 10 mV/s, 20 $^{0}$C, 0.05 M pH 4.55 Acetate Buffer.

### 3.2.2 Laccase electrochemical analysis

As laccase represents same characteristics as BOD, same characteristics should be observed during analysis of experiment results. However, due to spectrophotometric analysis results described before, it is clear that, laccase undergoes some disturbance while immobilized and loses its OR functions at almost 80-90%.

Laccase has higher rate of oxygen reduction while free (Figure 3.1 and Figure 3.2) compared to BOD, while BOD is not so affected by the immobilization procedure.

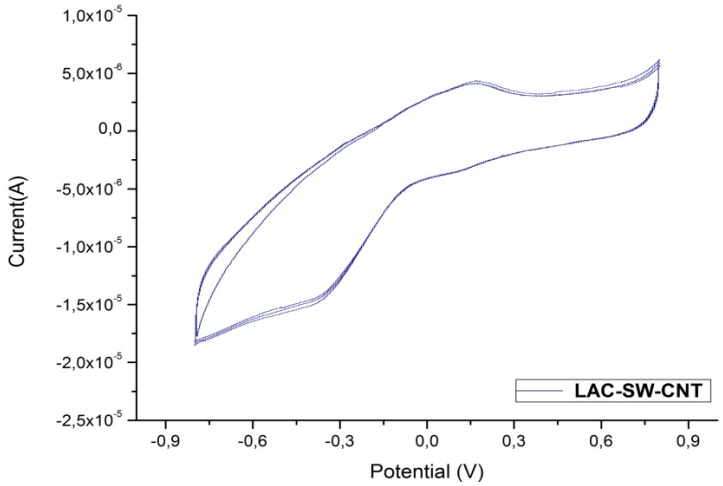


**A**

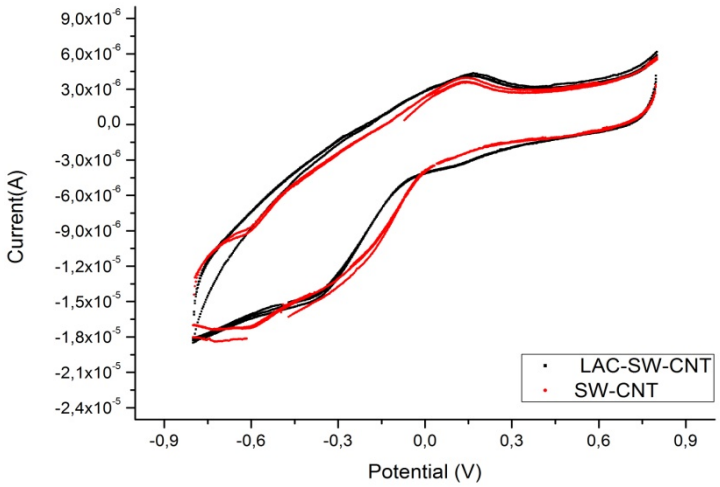


**B**

**Figure 3.6:** Cyclic voltammogram of (A) Laccase immobilized on SW-CNT (B) Laccase immobilized on SW-CNT and SW-CNT, 10 mV/s, 20 $^{o}$C, 0.05 M Acetate Buffer pH 4.55.

From the Figure 3.6 (A) it is possible to see that although laccase has both anodic and cathodic peaks at 0.2 V and 0.17 V respectively, the current of those peaks is very small meaning that only very small amount of laccase is really active on the surface of the electrode.

When compared to cyclic voltammogram of SW-CNT only, it is obvious that current values of anodic and cathodic peaks are 1-2 µA more than SW-CNT current peaks. Other widened zone means that there is some overpolarization, probably due to fact of thick and inactive laccase layer.

From the enzyme ORR process descriptions made in previous studies [27-29] it is concluded that ORR occur in two steps, meaning that in same manner as BOD ORR, Laccase will have two cathodic peaks. On the Figure 3.7, BOD and laccase cyclic voltammograms are compared; from this point it is very clear that BOD behaves better in direct immobilization state compared to laccase. Same conclusion was made also from spectrophotometric analysis of both enzymes. Both anodic and cathodic peaks of BOD are two times higher than laccase's ones.

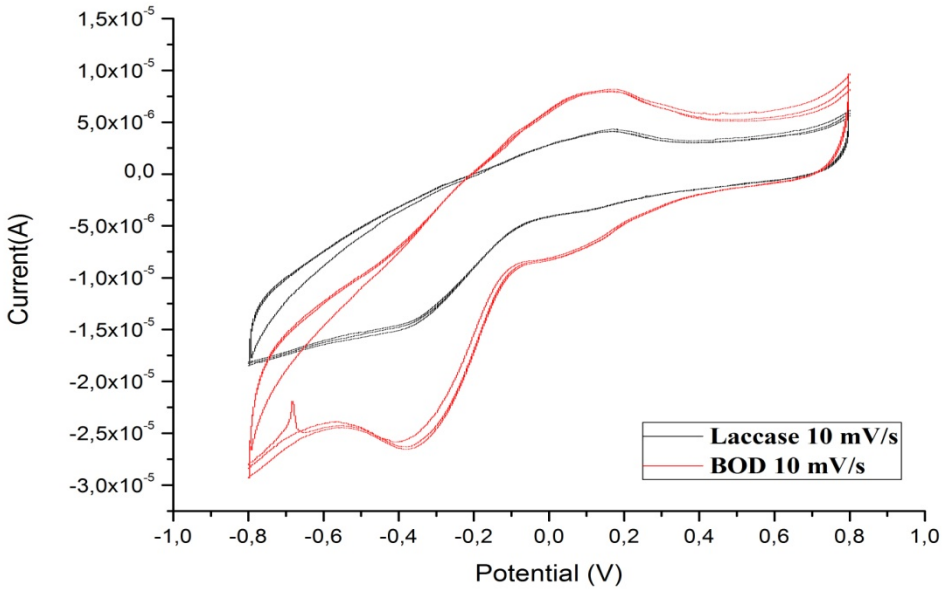


**Figure 3.7:** Cyclic voltammogram of) Laccase immobilized on SW-CNT and BOD immobilized on SW-CNT, 10 mV/s, 20 $^{o}$C, 0.05 M Acetate Buffer pH 4.55.

However, potential values of peaks stay the same. From this, it is concluded that although most of laccase loses its function when immobilized, the pattern of ORR stays the same as BOD.

To investigate the effect of PVP on the laccase immobilization cyclical voltammogram comparison was performed. From the Figure 3.8, it is seen that PVP modification of SW-CNT has no or negligible difference.

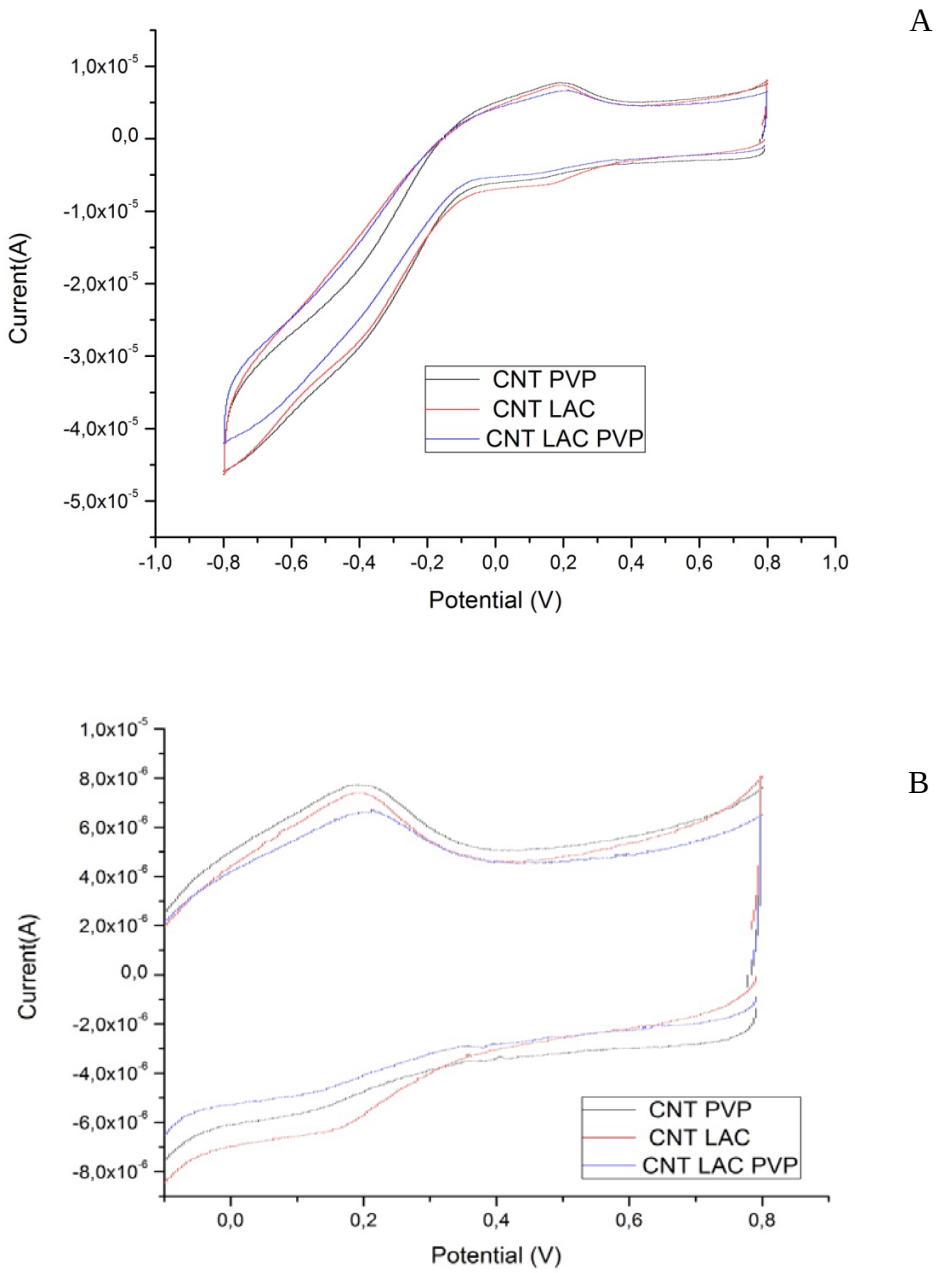


**Figure 3.8:** Cyclic voltammogram of various Laccase immobilization layouts (A) normal (B) zoomed, 10 mV/s, 20 $^{o}$C, 0.05 M Acetate Buffer pH 4.55

Three voltammograms follow almost the same pattern. Just SW-CNT-LAC layout shows slight peaks meaning that PVP even prevents diffusion of $O_2$ to electrode surface.

However, when we consider the effect of PVP on SW-CNT alone, it is a bit different case. Figure 3.9 shows that when SW-CNT is modified with PVP, there are some changes in the electrochemical behavior of SW-CNT. From the given cyclic

voltammogram, it is seen that there are shifts in both anodic and cathodic peaks, meaning that PVP at some stage interfere with ORR oxidation potential of SW-CNT. In addition, due to properties of PVP, there is a possibility that surface area of SW-CNT is modified. In a negative potential range, modified SW-CNT behaves differently: its current also becomes more negative.

Finally, it can be concluded that, although PVP modifies SW-CNT, it is unfavorable when enzyme is applied to this modification. One of the reasons can be that, enzyme is easily washed out from the surface, or electron tunneling system of enzyme is "clotted" by PVP presence.

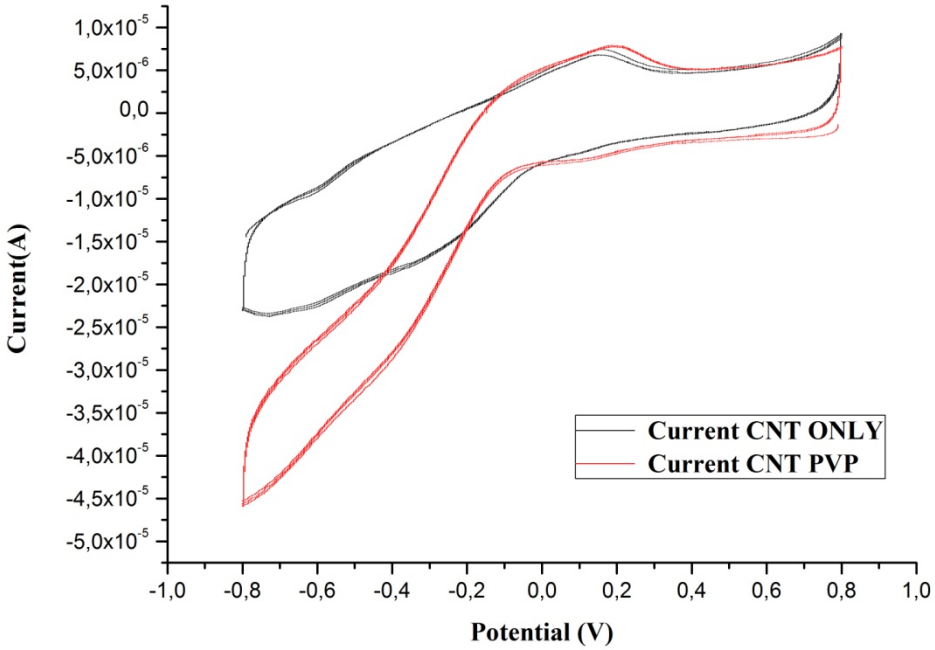


**Figure 3.9:** Cyclic voltammogram of SW-CNT modification by PVP, 10 mV/s, 20 $^{o}$C, 0.05 M Acetate Buffer pH 4.55.

### 3.2.3 Effectiveness Calculation

In order to calculate efficiency of an enzyme from the cyclic voltammogram, Randles-Sevcik equation **(3.1)** should be used. However, it is not possible to address to real values of current equation. One of the reasons for this is that enzymes do not have active surface area as conventional catalysts do.

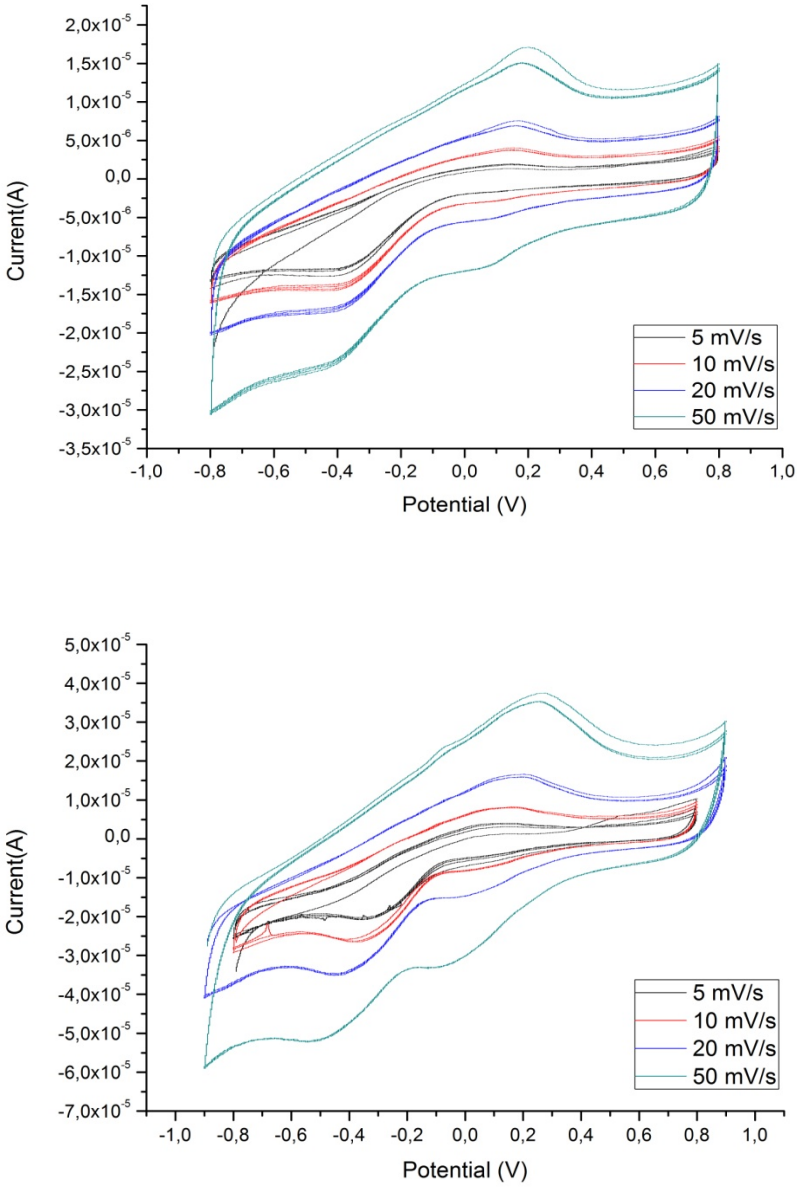


**Figure 3.10:** Comparison of sweep rate with current peaks of Laccase (up) and BOD (bottom), 20 $^{o}$C, 0.05 M Acetate Buffer pH 4.55.

$$i_p = 2.69\times10^5\, n^{3/2}\, A\, D^{1/2}\, C\, v^{1/2} \qquad \textbf{(3.1)}$$

Instead, each enzyme can process one reaction at a time, and its surface has nothing to do with its efficiency [26, 27, 28]. From previous studies source [30, 32], it is clear that in process of ORR clusters of Cu atoms participate while surface of an enzyme stays inactive.

As a result of modifications made in Randles-Sevcik equation, instead of active area (A), we can use an enzyme efficiency or enzyme ORR coefficient. For both Laccase and BOD, number of transferred electrons is 4 [29]. To proceed with further calculations, Randles-Sevcik equation should be implemented on the plot.

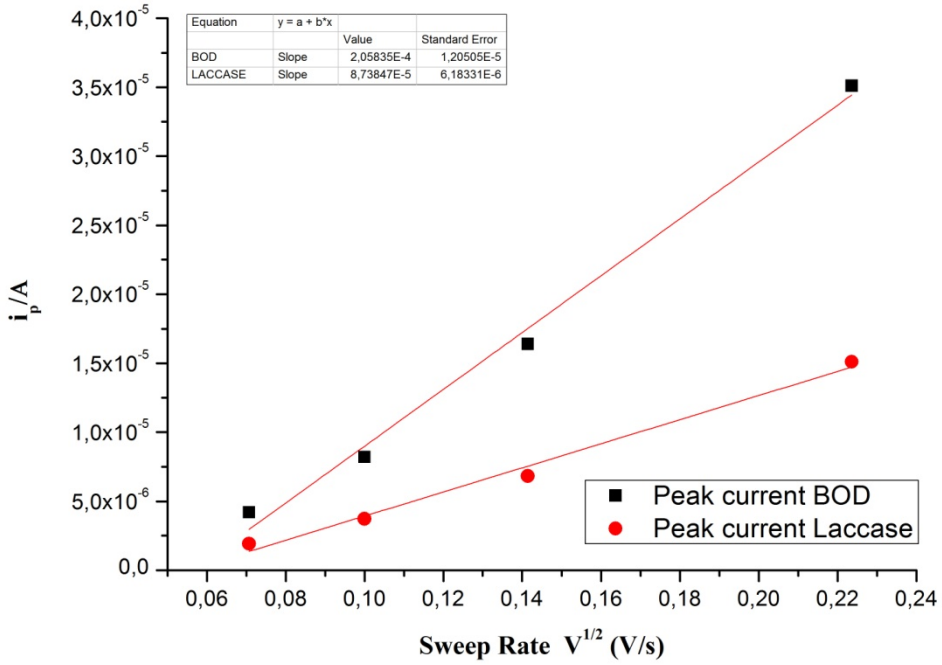


**Figure 3.11**: Randles-Sevcik plot for BOD-SW-CNT and laccase-SW-CNT layouts, 0.05 M Acetate Buffer pH 4.55.

From the Figure 3.11, it is concluded that slope of BOD and laccase equals to $2{,}06x10^{-4}$ and $8{,}74x10^{-5}$ respectively. Considering that experiment is performed at the same conditions, it becomes clear that values D, n and C are equal for both BOD and laccase. ORR efficiency of BOD is approximately 2.35 times efficiency of laccase. When compared to spectrophotometric results, where BOD reached its maximum absorbance in 110 minutes, while laccase reached its maximum absorbance in 250 minutes it is clear that efficiency is approximately 2.27. That means that results of enzyme efficiency calculations using spectrophotometric tools and electrochemical tools are the same.

### 3.2.4 Hydrogen peroxide effect in Laccase-SW-CNT layout

To increase amount of oxygen in the electrolyte, it was decided to add hydrogen peroxide into it. Hydrogen peroxide oxidation occurs according to the following reaction:

$$H_2O_2 \rightarrow O_2 + 2H^+ + 2e^- \qquad E_v = +0.68\ V$$

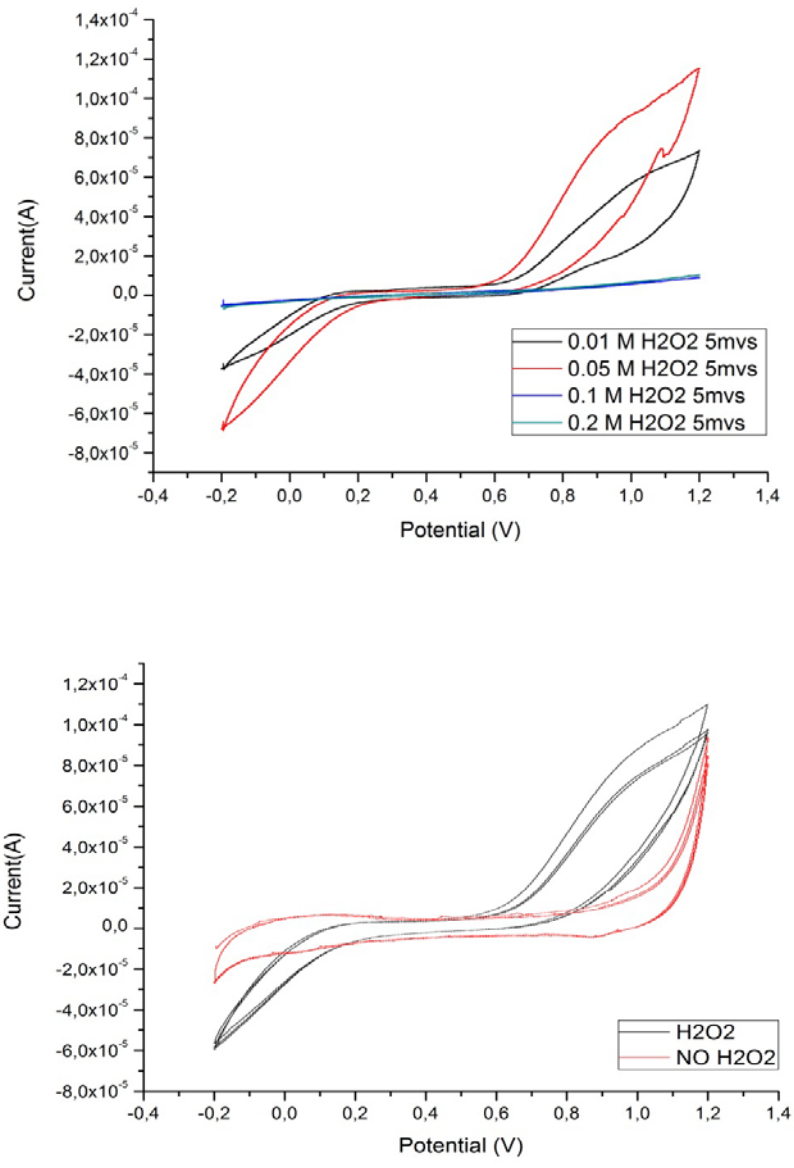


**Figure 3.12:** Effect of $H_2O_2$ on Laccase-SW-CNT cathode, 20 $^oC$, 0.05 M Acetate Buffer pH 4.55.

Hydrogen peroxide not only provides $O_2$ to electrolyte, but also fills it with electrons that are essential for further ORR. In addition it is thermodynamically favorable

reaction. In the Figure 3.12, cyclic voltammograms of electrolytes with various amounts of $H_2O_2$ in electrolyte are given.

Although hydrogen peroxide changes the behavior of the LAC-SW-CNT (no peaks observed), it is clear that reaction undergoing there is strictly related to H2O2 itself but not to Laccase or CNT structure. Meaning that, hydrogen peroxide interferes with ORR reactions of electrode [27]. At higher concentrations, hydrogen peroxide totally inhibits all reactions on the electrode, or probably just removes the absorbed layout from electrode surface.

### 3.2.5 Enzyme kinetics comparative analysis

From both spectrophotometric and electrochemical results, it was obtained that both measurement techniques are useful. However, an essential part of the whole experiment is to prove it quantitatively. In order to make it, some main terms should clearly be understood. After fitting Randles-Sevcik equation (3.1) to enzyme kinetics, it is possible to make comparative analysis of the equation for both laccase and BOD. In enzymes, there is no effect of double layer, as substrates enter enzyme and oxidized by its metallic active centers one by one.

As first step, some assumptions should be made. Firstly, it should be assumed that enzyme catalyzed reaction rate follows Michaelis-Menten type kinetics. Secondly, it should be assumed that enzymes are evenly distributed on the surface of a nonporous support material and all enzyme molecules are equally active. Thirdly, it should be assumed that substrate diffuses through a thin liquid film surrounding the support surface to reach the reactive surface. Finally, it should be assumed that the process of immobilization has not altered the enzyme structure and the intrinsic parameters (Vm, Km) remained unchanged.

Implementing results in Damköhler numbers (Da) (3.2) equation, that describes the significant effect of external diffusion resistance on the rate of enzyme reaction it is possible to understand the limitng step in the overall enzyme ORR.

$$Da = \frac{maximum\ rate\ of\ \ reaction}{maximum\ rate\ of\ \ diffusion} = \frac{V_m'}{k_L [S_b]} \qquad \textbf{(3.2)}$$

Where Vm' is the maximum reaction rate per unit of external surface area (e.g. g/cm2-s), $k_L$ is the liquid mass transfer coefficient (cm/s) and $S_b$ is the substrate concentration in bulk solution (g/cm3). If Da >> 1, the external diffusion rate is limiting; Da << 1, the reaction rate is limiting; Da ≈ 1, the external diffusion and reaction resistances are comparable.

The maximum rate of reaction and rate of the diffusion can be taken from spectrophotometric results. Maximum rate of reaction is assumed to be the free enzyme reaction kinetics, while rate of diffusion is the only factor that defines the reaction of an enzyme when it is immobilized on the surface of the electrode. From given information and both enzyme ABTS oxidation graphs, it can be concluded that, for laccase the Da value equals to 20,83 and for BOD the Da value is 4,07. In both cases Da number represents dependence of the reaction rate on the external diffusion rate. Given values show that, laccases is more strictly depends on the spatial location and position towards electrode surface than BOD. In this case, whatever enzymes maximum rate, when immobilized it will be equal to diffusion rate of the substrate.

Returning to immobilized enzyme systems, it is essential to underline that the overall production rate is determined by: liquid film mass transfer (external diffusion) of a substrate or product, intraparticle mass transfer (internal diffusion) of a substrate, product in porous supports and enzyme catalysis reaction [32-40].

If the external diffusion rate (g/cm2-s) (3.3) can be described in the following equation;

$$J_s = k_L([S_b] - [S_s]) \tag{3.3}$$

where $k_L$ is the liquid mass transfer coefficient (cm/s), $S_b$ is the substrate concentration in bulk solution ($g/cm^3$) and $S_s$ is the substrate concentration on the surface of an enzyme. And the production rate formation (3.4) is described by the following equation;

$$v' = \frac{V_m'[S_s]}{K_m + [S_s]} \tag{3.4}$$

where $V_m$' the maximum reaction rate per unit surface area ($g/cm^2$-s). At the steady state conditions, these two equations will be equal to each other meaning that, previous assumption that activity coefficient or reaction rate is equal to diffusion rate of substrate towards enzyme film [15-25].

From the previous data, spectrophotometrically the activity ratio of immobilized laccase to immobilized BOD is 1:2.27 respectively, electrochemically the activity ratio of immobilized laccase to immobilized BOD is 1:2.35 respectively.

### 3.2.6 Loss of function of Enzymes

Although through research, it was obvious that enzyme modification does not obey conventional laws of electrochemistry, it is essential to emphasize that loss of enzymes activity was very fast and there were huge difference between enzyme on first day of use and on fifth day of use (Fig 3.14).

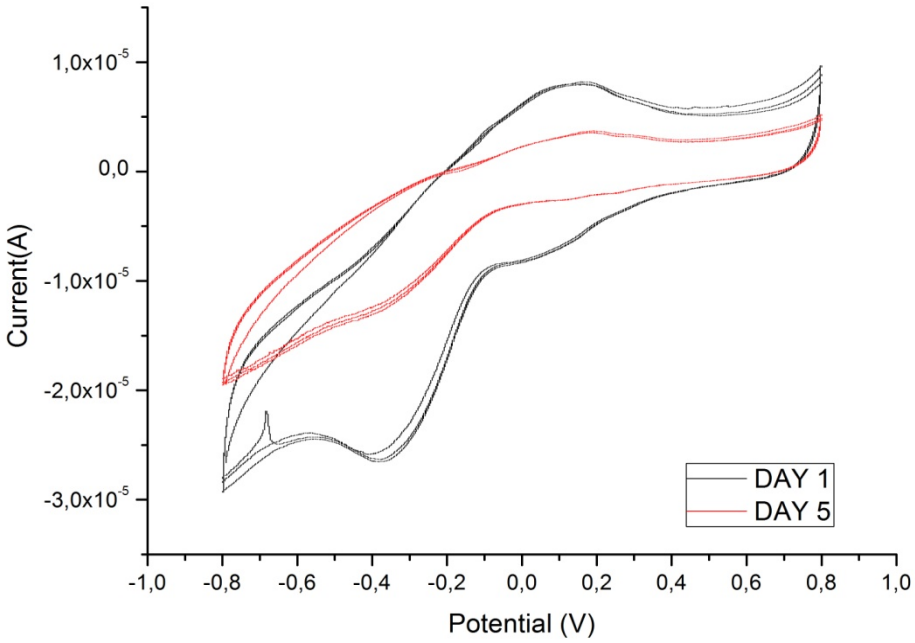


**Figure 3.13:** BOD activity drop, SW-CNT-BOD layout, 20 $^oC$, 0.05 M Acetate Buffer pH 4.55, 10 mV/s.

## 4. CONCLUSION AND RECOMMENDATIONS

A research was performed to develop and analyze enzymatic activity as biocatalyst on the surface of the cathode for oxygen reduction reactions. To increase the active surface area and stimulate electron tunneling properties for electrode single walled carbon nanotubes were utilized.

As enzymes strictly depend on their position towards electron and substrate, both laccase and bilirubin oxidase activity were investigated under immobilized conditions and free in solution. Firstly, it was identified although laccase exhibits excellent reductive ability while free in solution; its efficiency dramatically falls down when immobilized. Bilirubin oxidase shows better ectivity while immobilized. Hypothesis was proved both spectrophotometrically and electrochemically. The correlation of activities of bilirubin oxidase and laccase exhibit same value after both techniques of proof. However, there is a current peak shift occurs to enzymes when compared it to literature values.(200 mV vs 500 mV vs. NHE). This phenomenon can be caused by various factors, beginning from activity differences of enzymes and ending at low solubility of oxygen in given electrolyte.

Hydrogen peroxide was used to stimulate formation of oxygen and fill electrolyte with it. However, it interrupted with enzyme kinetics and probably removed layer from electrode.

When compared to the conventional fuel cells, enzyme fuel cells have lower ovelpolarization but also exhibit low currents. This can be improved using special mediators or polymer stimulators. High current densities for O2 reduction were achieved by Heller and co-workers when laccase or bilirubin oxidase was embedded into redox hydrogel polymers that contained Os-pyridine complexes. That complex generated high ratio of polymer-bound Os atoms to enzyme molecules. However, it is still uncertain whether high current profiles arise from enzymes or polymers-Os structures [33].

Another way to modify current outcome is by using genetic manipulation. As it was mentioned before, TvL T-1 coppers trigonal coplanar coordination differes from other bmCuOs that have 4-fold structure. So it was considered axial coordination of T1-copper was the reason for high-redox potentials. When TvL T1 is compared to C.cinereus laccase (CcL), there is a difference in redox potential of 550 mV that probably arises from axial position of T1 coppers. In TvL T1 it is occupied by phenylalanine while in CcL T1 it is occupied with leucine. Consequently, in next studies mutational modifications can be made to amino acid components of enzymes and changes in current values can be observed. Probably, this can improve efficiency of enzyme fuel cells [37-42].

## REFERENCES


[1] **Her**, **M.L.** (2006). Redox properties, electrochemistry of oxygen, in Encyclopedia of Electrochemistry: Inorganic Electrochemistry, ed. A. J. Bard, M. Stratman, F. Scholz, C. J. Pickett, Wiley-VCH, Weinheim, vol. 7a, pp. 119–142.

[2] **Bullen, R.A., Arnot, T.C., Lakeman J.B.,** (2006). Walsh, Biofuel cells and their development, Biosensors and Bioelectronics, pp. 2015-2045.

[3] **Vaz-Dominguez, C., Campuzano, S., Rudiger, O., Pita, M., Gorbacheva, M., Shleev, S., Fernandez, V. M., Lacey, A.L.D., (**2008). Laccase electrode for direct electrocatalytic reduction of O2 to H2O with high-operational stability and resistance to chloride inhibition, Biosensors and Bioelectronics, pp. 531-537.

[4] **Bullen, R.A., Arnot, T.C., Lakem J.B., Walsh, F.C.,** (2006). Biofuel cells and their development, Biosensors and Bioelectronics, pp. 2015-2045.

[5] **Li, W., Liang, C., Qui, J., Zhou, W., Han, H., Wei, Z., Sun, G., Xin, Q.,** (2002). Carbon Nanotubes as Support for Cathode Catalyst of a Direct Methanol Fuel Cell. *Carbon*. Vol. **40**, no. 5, pp. 791-794.

[6] **Tayhas, G., Palmore, R., Kim, H.H.** (1999). Electro-enzymatic reduction of dioxygen to water in the cathode compartment of a biofuel cell, Journal of Electroanalytical Chemistry, pp. 110-117.

[7] **Logan, B.E., Hamelers, B., Rozendal, R., Schröder, U., Keller, J., Freguia, S., Aelterman, P., Verstraete W., and Rabaey, K.**, (2006). Microbial fuel cells: methodology and technology, Environmental Science and Technology, pp. 307-314

[8] **Liu, Z.-D., Li, H.-R.,** (2007). Effects of bio- and abio-factors on e lectricity production in a mediatorless microbial fuel cell, Biochemical Engineering Journal, pp. 209-214.

[9] **Palmore, GTR., Kim, HH.,** (1999). Electro-enzymatic reduction of dioxygen to water in the cathode compartment of a biofuel cell. J Electroanal Chem464, pp.110–117.

[10] **Mano, N., Kim, H.-H., Heller, A., (**2002). On the relationship between the characteristics of bilirubin oxidases and O2 cathodes based on their"wiring", J. Phys. Chem. B 106, pp. 8842–8848

[11] **Tan, Y., Deng, W., Ge, B., Xie, Q., Huang, J., Yao, S.** (2009). Bio fuel cell and phenolic biosensor based on acid-resistant laccase-glutaraldehyde functionalized chitosan-multiwalled carbon nanotubes nanocomposite film. BiosensBioelectron **Vol. 24**, pp. 2225–223.

[12] **Lefebvre, O., Ooi, W.K., Tang, Z., Abdullah-Al-Mamun, Md., Chua, H.Y.** (2009). Ng, Optimization of a Pt-free cathode suitable for practical applications of microbial fuel cells, Bioresource Technology, pp. 4907-4910

[13**] Wang, J., Liu, G., Jan**, **M.R.,** (2004). Ultrasensitive electrical biosensing of proteins and DNA:carbon nanotube derived amplification of the recognition and transductionevents, J. Am. Chem. Soc. 126, pp.3010–3011.

[14] **Pardo, A., Basseguy, R., Bergel, A.**, (2006). Simple design of cast myoglobin /polyethylenei-mine modified electrodes, J. Appl. Electrochem. 36, pp.835–842

[15] **Ivnitski, D., Atanassov, P.,** (2007). Electrochemical studies of intramolecular electrontransfer in laccase from Trametes versicolor, Electroanalysis 19, pp.2307–2313.

[16] **Shleev, S., Tkac, J., Christenson, A., Ruzgas, T., Yaropolov, A.I., Whittaker, J.W., Gorton, L.** (2005). Direct electron transfer between copper-containing proteins and electrodes,Biosens.Bioelectron. **vol. 20**, pp. 2517–2554

[17] **Sakurai, T., Suzuki, S.** (1997). Spectroscopy of cucumber ascorbate oxidase and fungallaccase, in: A. Messerschmidt (Ed.), Multi-Copper Oxidases, World Scientifi c,Singapore, pp. 225–250

[18] **Solomon, E.I., Sundaram, U.M., Machonkin, T.E., (**1996). Multicopper oxidases andoxygenases, Chem. Rev. 96, pp.2563–2605

[19] **Mandal, S., Kazmi, N.H., Sayre, L.M.** (2005). Ligand dependence in the copper-catalyzedoxidation of hydroquinones, Arch. Biochem. Biophys. pp.435 21

[20] **Ammam, M., Fransaer, J.. (**2010). Micro-biofuel cell powered by glucose/O2 based on electro-deposition of enzyme, conducting polymer and redox mediators: Preparation, characterization and performance in humanserum. Biosens Bioelectron **Vol. 25**, pp.1474–1480

[21] **Ammam, M., Fransaer, J.. (**2010). Glucose microbiosensor based on glucose oxidase immobilized by AC-EPD: Characteristics and performance inhuman serum and in blood of critically ill rabbits. Sens Actuators BChem 145, pp.46–53

[22] **Cumpson, P.J., Briggs, D., Grant, J.T.** (2003). Surface Analysis by Auger and X-ray Photo electron Spectroscopy, IM publications and Surface Spectra Limited, Chichester:Manchester, Chapter Angle-Resolved X-Ray Photoelectron Spectroscopy

[23] **Shim, M., Javey, A., Kam, N.W.S, Dai, H.** (2001). Polymer functionalization for air-stable n-type carbon nanotube field-effect transistors, J. Am. Chem. Soc.123, pp.11512–11513

[24] **Bradley, K., Briman, M., Star, A., Gruner, G.** (2004).Charge transfer from adsorbed proteins,Nano. Lett. 4, pp.253-256

[25] **Farver, O., Pecht, I. (**1991). Electron transfer in proteins: in search of preferential pathways, FASEB J. 5, pp.2554–2559

[26] **Tsujimura, S., Kuriyama, A., Fujieda, N., Kano, K., Ikeda**, **T.**(2005). Mediated spectroelec-trochemical titration of proteins for redox potential measurements by a separator-less one-compartment bulk electrolysis method,Anal.Biochem.337, pp.325–331.

[27] **Rusling, J.F., Forster, R.J. (**2003). Electrochemical catalysis with redox polymer rand poly ion-protein films, J. Col. Intreface Sci, 262, pp.1–15.

[28] **Armstrong**, **F.A.** (2002). Insights from protein film voltammetry into mechanism of complexbiological electron-transfer reactions, J. Chem. Soc., Dalton Trans, pp.661–671

[29] **Zoppellaro, G., Sakurai, N., Kunishige, K., Sakurai, T. (**2004). The reversible change in the redox state of T1 Cu in Myrothecium verrucaria bilirubin oxidase, Biosci.Biotechnol.Biochem. 68, pp.1998–2000

[30] **Armstrong, F.A. (**2005). Recent developments in dynamic electrochemical studies of adsorbed enzymes and their active sites, Curr.Opin.Chem.Biology 9, pp.110–117

[31] **Weigel, M.C., Tritscher, E., Lisdat, F.** (2007). Direct electrochemical conversion of bilirubinoxidase at carbon nanotube-modified glassy carbon electrodes, Electrochem.Commun. 9, pp.689-693

[32] **Leger, C., Elliott, S.J., Hoke, K.R., Jeuken, L.J.C., Jones, A.K., Armstrong**, **F.A.** (2003). Enzyme electro kinetics: Using protein film voltammetry to investigate redox enzymes and their mechanisms, Biochemistry 42 pp.8653.

[33] **Zhao, L., Liu, H., Hu**, **N.** (2006). Assembly of layer-by-layer films of hemeproteins and single-walled carbon nanotubes: electrochemistry and electrocatalysis, Anal Bioanal.Chem. 384, pp.414–422

[34] **Kang, C., Shin, H., Heller**, **A.** (2006). On the stability of the “wired”bilirubin oxidase oxygen cathode in serum, Bioelectrochemistry 68 (68), pp.22–26

[35] **Xu, F., Shin, W., Brown, S.H., Wahleithner, J.A., Sundaram, U.M., Solomon, E.I.** (1996). A study of a series of recombinant fungal laccases and bilirubin oxidase that exhibit significant differences in redox potential, substrate specificity, and stability ,Biochim. Biophys. Acta 1292, pp.303–311

[36] **Bourbonnais, A., Robert, D., Leech, S., Dónal P., Michael, G.** (1998). "Electrochemical analysis of the interactions of laccase mediators with lignin model compounds", Biochimica et Biophysica Acta (BBA) - General Subjects 1379 (3): pp. 381–390

[37**] Haaf, A., Sanner, F., Straub**, **F.** (1985). "Polymers of N-Vinylpyrrolidone: Synthesis, Characterization and Uses". Polymer Journal 17 (1): pp. 143–152.

[38] **Allen. J., Larry, R.**(2002). Electrochemical Methods: Fundamentals and Applications (2 ed.). Wiley. ISBN 0-471-04372-9.

[39] **Tsujimura, S., Kano, K., Ikeda, T.** (2005). Bilirubin oxidase in multiple layers catalyzes four-electron reduction of dioxygen to water without redox mediators, J. Electroanal.Chem. 576, pp.113–120.

[40] **Lim, J., Malati, P., Bonet, F., Dunn**, **B.** (2007). Nanostructured sol–gel electrodes for biofuelcells, J. Electrochem. Soc. 154 A140–A145

[41] **Quan, D., Kim, Y., Shin**, **W.** (2004). Characterization of an amperometric laccase electrode covalently immobilized on platinum surface, J. Electroanal. Chem. 561,pp. 181–189

[42] **Zheng, W., Li, Q., Su, L., Yan, Y., Zhang, J., Mao, L.** (2006). Direct electrochemistry of multi-copper oxidases at carbon nanotubes noncovalently functionalized with cellulosederivatives, Electroanalysis 18 ,pp. 587–594

**CURRICULUM VITAE**

**Name Surname:** Ilyas Dzhabarly

**Birth Date:** 07.08.1985

**Address:** Mahmut Şevket Paşa Mh.Aslan Sk.16 D 4 Istanbul

**E-Mail:** kredo777@msn.com

**B.Sc.:** Istanbul Technical University Molecular Biology and Genetics